



HAL
open science

Single-particle tracking photoactivated localization microscopy of membrane proteins in living plant tissues

Vincent Bayle, Jean-Bernard Fiche, Claire Burny, Matthieu Pierre Platre, Marcelo Nollmann, Alexandre Martinière, Yvon Jaillais

► **To cite this version:**

Vincent Bayle, Jean-Bernard Fiche, Claire Burny, Matthieu Pierre Platre, Marcelo Nollmann, et al.. Single-particle tracking photoactivated localization microscopy of membrane proteins in living plant tissues. *Nature Protocols*, Nature Publishing Group, 2021, 16 (3), pp.1600-1628. 10.1038/s41596-020-00471-4 . hal-03153046

HAL Id: hal-03153046

<https://hal.archives-ouvertes.fr/hal-03153046>

Submitted on 26 Feb 2021

HAL is a multi-disciplinary open access archive for the deposit and dissemination of scientific research documents, whether they are published or not. The documents may come from teaching and research institutions in France or abroad, or from public or private research centers.

L'archive ouverte pluridisciplinaire **HAL**, est destinée au dépôt et à la diffusion de documents scientifiques de niveau recherche, publiés ou non, émanant des établissements d'enseignement et de recherche français ou étrangers, des laboratoires publics ou privés.

Single-particle tracking Photo-Activated Localization Microscopy of membrane proteins in living plant tissues.

Vincent Bayle^{1*}, Jean-Bernard Fiche^{2*}, Claire Burny^{3,4}, Matthieu Pierre Platre¹, Marcelo Nollmann², Alexandre Martinière^{5#} and Yvon Jaillais^{1#}

¹ Laboratoire Reproduction et Développement des Plantes, Université de Lyon, ENS de Lyon, UCB Lyon 1, CNRS, INRAE, F-69342 Lyon, France.

² Centre de Biochimie Structurale, Centre National de la Recherche Scientifique Unité Mixte de Recherche 5048, Institut National de la Santé et de la Recherche Médicale U1054, Université de Montpellier, 34090 Montpellier, France.

³ Institut für Populationsgenetik, Vetmeduni Vienna, Vienna, Austria

⁴ Vienna Graduate School of Population Genetics, Vetmeduni Vienna, Vienna, Austria.

⁵ BPMP, Univ Montpellier, CNRS, INRAE, Montpellier SupAgro, Montpellier, France

*equal contribution

corresponding authors: alexandre.martiniere@cnrs.fr; yvon.jaillais@ens-lyon.fr

KEYWORDS super-resolution microscopy, plants, molecular diffusion, single particle tracking, single molecule localization microscopy, photo-activated localization microscopy, sptPALM, total internal reflection fluorescence microscopy, root, Rho GTPase, auxin

EDITORIAL SUMMARY This protocol describes how to perform single-particle tracking Photo-Activated Localization Microscopy (sptPALM) of membrane proteins in living plant tissues. The procedure covers all stages from sample preparation to data analysis.

TWEET A new Protocol for single particle tracking Photo-Activated Localization Microscopy (sptPALM) of membrane proteins in live plant tissues. #PALM #super-resolution @YvonJaillais @RDPlab

COVER TEASER sptPALM of membrane proteins in live plant tissues

Abstract. Super-resolution microscopy techniques have pushed the limit of optical imaging to unprecedented spatial resolutions. However, one of the frontiers in nanoscopy is its application to intact living organisms. Here we describe the implementation and application of super-resolution single-particle tracking Photo-Activated Localization Microscopy (sptPALM) to probe single-molecule dynamics of membrane proteins in live roots of the model plant *Arabidopsis thaliana*. We first discuss the advantages and limitations of sptPALM for studying the diffusion properties of membrane proteins and compare this to fluorescence recovery after photobleaching (FRAP) and fluorescence correlation spectroscopy (FCS). We describe the technical details for handling and imaging the samples for sptPALM, with a particular emphasis on the specificity of imaging plant cells, such as their thick cell walls or high degree of autofluorescence. We then provide a practical guide from data collection to image analyses. In particular, we introduce our sptPALM_viewer software and how to install and use it for analyzing sptPALM experiments. Finally, we report a R statistical analyses pipeline to analyze and compare sptPALM experiments. Altogether, this protocol should enable plant researchers to perform sptPALM using a benchmarked reproducible protocol. Routinely, the procedure takes 3-4 hours of imaging followed by 3-4 days of image processing and data analysis.

Introduction

Biological membranes are, in general, fluid¹ and allow for lateral diffusion of protein and lipid components in 2-dimensions within the membrane plane². This lateral mobility is critical for the functions of both proteins and lipids. Indeed, lateral mobility is an important parameter in membrane-based reactions, as it plays a prominent role in the lateral segregation of molecules in distinct membrane domains and in phase separation processes². It is thus of utmost importance to quantitatively measure proteins dynamics within biological membranes *in vivo*. Measuring molecule diffusion in live specimens is technically difficult, particularly in plant tissues, which contain highly turgid cells encapsulated in a thick cell wall³. In addition, plants are rich in highly autofluorescent molecules, both inside the cell and in the cell wall (e.g. chlorophyll, phenols, flavonoids, tannins, anthocyanins, lignin, suberin)⁴. In recent years, several advanced microscopy

techniques, compatible with plant tissue imaging, emerged to estimate or measure molecular diffusion within membranes, including fluorescence recovery after photobleaching (FRAP), fluorescence correlation spectroscopy (FCS) and single-particle tracking (SPT)^{2,5-21}. Here, we report a detailed protocol for single-particle tracking analysis using photo-activated localization microscopy (sptPALM). We describe the principle of the sptPALM method and how it can be implemented in live plant tissues. We also discuss the advantages and limitations of sptPALM compared to other techniques used to probe molecular diffusion in plants.

sptPALM was first proposed by Manley et al. as a live single-molecule imaging technique aiming at describing the dynamic behavior of single molecules, including their localization and diffusion^{22,23}. sptPALM is based on a temporal separation of fluorescent emitters, which is achieved by photo-activation or photo-conversion of fluorescent objects induced with low light intensity²² (**Fig. 1a-b**). This strategy allows that only a small fraction of the fluorescent molecules is stochastically activated, and therefore photo-activated/converted molecules are well separated from each other during imaging²². This is preventing Airy disk overlap from single emitters, which can then be fitted with high accuracy, typically with ~30 nm lateral resolution^{22,24,25}. Hence, this technique belongs to the super-resolution imaging methods, as it breaks the diffraction barrier (Abbe limit in resolution)²⁶. In sptPALM, photo-activated/converted single molecules are continuously imaged at a high acquisition rate (>50Hz) using a laser beam adapted to the respective excitation wavelength, in order to probe diffusion behavior. Because this time-lapse acquisition is performed in live samples, with molecules diffusing during the time-lapse acquisition, and photo-activated/converted molecules are not immediately photo-bleached during acquisition (due to excitation with mild laser intensity), this technique allows to track the positions of single molecules through time before the photo-activated/converted fluorescent emitter is bleached (or moves out of focus) (**Fig. 1c**)²². This technique thereby allows us to obtain the trajectories of single molecules with a xy resolution of ~30nm. However it does not improve the axial resolution (i.e. depth in z), which is determined in our experimental set-up by the depth of the evanescent wave¹⁴. Note that the z-position of fluorescent emitters can be resolved with higher accuracy by using additional methods (not discussed hereafter) based on astigmatic or engineered point spread functions (PSF)²⁷⁻³¹. From single molecule tracks, it is then possible to obtain a range of quantitative parameters, including a spatial map of the trajectories, their diffusion coefficient, their molecular displacement, their

diffusion type (active, Brownian or constrained), and their transition state (between the different diffusion types)²³.

Development of the protocol

Single-particle tracking experiments have traditionally been performed on proteins tagged with classical Fluorescent Proteins (FP)⁸. In this case, since all FPs are excited simultaneously, a single ensemble of molecules (e.g. plasma membrane domains, compartments, clathrin-coated pits, ...) is imaged and tracked over time. SPT methods have recently been used to address biological questions in the field of plant cell biology, development and environmental adaptations^{5-8,12,13,32-39}.

Photo-convertible proteins have first been used by Manley and colleagues²² to track single molecules in live-cells, introducing the sptPALM imaging technique. As compared to SPT experiments performed with regular FPs, sptPALM provides information on the diffusion of single molecules. This is an important distinction since the dynamic of single molecules can sometimes show different behavior than their associated structure within the cell. For example, we found that the clathrin light chain 2 (CLC2) shows static punctuated structures at the membrane with very little lateral diffusion when observed with classical FP and tracking analyses⁴⁰⁻⁴². In contrast, at the molecular level assessed by sptPALM, we observed that a fraction of CLC2 molecules are diffusing within the membrane¹⁵.

To develop our sptPALM protocol in plants, we adapted the sample preparation for sptPALM experiments using total internal reflection fluorescence microscopy/variable-angle epifluorescence microscopy (TIRF/VAEM). Our work built on previous efforts for TIRFM/VAEM imaging in plants, which is made difficult by the presence of the cell wall between the coverslip and the plasma membrane^{6,8,40,43,44}. However, we describe how to handle the samples for root imaging in order to have reproducible results (see Experimental design section sample preparation). Second, we optimized the acquisition conditions to obtain the

longest tracks possible while maintaining a good precision of localization and we developed an acquisition protocol to obtain reproducible and statistically-sound results (see Experimental design section Choice of microscope and considerations for image acquisition). Third, we developed an analysis pipeline for image post-processing. For this image analyses pipeline, we took advantage of previously published software for single-particle tracking (MTT or TrackMate)^{45,46} and designed a software-package that we call “sptPALM_viewer”, to analyze the tracks and compile the data^{14,15} (<https://github.com/jbfiche/sptPALM>) (for details see Experimental design sections Image analysis - Detection and reconnection and Image analysis - Calculation of the mean square displacement and instantaneous diffusion).

Overview of the Procedure

The Procedure described in this protocol consists of five main stages. First, we describe how to prepare the samples, including descriptions of coverslip cleaning (Steps 1-8), plant culture (Step 9) and sample preparation (Steps 10-13). Second, we provide guidelines for image acquisition, including how to set-up the microscope parameters (Steps 14-25), to assess single molecule localization (Steps 26-28), and to check false-positive detections and minimize background fluorescence (Steps 29-34). Third, we describe how to detect and localize the position of fluorescent emitters and track them through time using published tracking software (i.e. MTT or TrackMate^{45,46}) (Steps 35 to 53) and to compile these data using our “sptPALM_viewer” (Steps 54 to 55). Fourth, we explain how to use the “sptPALM_viewer” to filter the tracks and to estimate molecule diffusion (Steps 56-62). Fifth, we propose an R-based statistical pipeline for the quantitative analysis of the diffusion data (Steps 63-66).

Applications of the method

We have used sptPALM to study the localization and dynamics of plasma membrane-localized proteins and lipids in *Arabidopsis*, including the RHO GTPase RHO-OF-PLANTS6 (ROP6), the aquaporin PLASMA MEMBRANE INTRINSIC PROTEIN2;1 (PIP2;1), the P-type ATPase (AHA2), the small integral protein LOW TEMPERATURE INDUCIBLE6b (LTI6b), CLATHRIN-LIGHT CHAIN (CLC2) and a sensor for the plasma membrane-localized lipid phosphatidylserine (PH^{EVECTIN2})^{14-16,21}. Using these diverse arrays of proteins, we detected

distinct diffusion behavior in the plane of the plant plasma membrane. We found proteins, such as LTI6b, which are largely mobile molecules within the plasma membrane (D around $0.1 \mu\text{m}^2/\text{s}$, with D the diffusion coefficient - note that all log-values mentioned in this manuscript refer to \log_{10} -transformed values which you can back-transform using $10^{\log_{10}(D)}$ ^{15,16}). By contrast, we found proteins, such as PIP2;1 or AHA2, that are highly confined (i.e. D around $0.001 \mu\text{m}^2/\text{s}$)^{15,16}. In addition, some proteins, such as the phosphatidylserine sensor or the clathrin light chain CLC2 harbor two distinct subpopulations of molecules, one mobile and one immobile^{14,15}. Finally, we also found some examples of proteins with distinct diffusion dynamics in response to a given stimulus. For example, ROP6 is largely mobile in the absence of treatment, but about 25-30% of ROP6 molecules become immobile rapidly after treatment with the plant hormone auxin¹⁴, or after osmotic stress²¹. Importantly, the distinct mobility of a subpopulation of ROP6 in response to auxin or osmotic stress appears to be linked with the signaling activity of this small GTPase^{14,21}. Accordingly, a constitutive active mutant of ROP6 (ROP6^{CA}), which is locked in its GTP-bound active conformation, also harbors about 30% of immobile molecules even in the absence of auxin treatment¹⁴.

While our method was applied to membrane proteins, including transmembrane proteins, lipid-binding proteins, and lipid-anchored proteins, we expect that it could be easily implemented to analyze the localization of other proteins in the vicinity of the cell surface such as cytoskeleton or cell wall components. In fact, we successfully applied our sptPALM technique to image the TONOPLAST INTRINSIC PROTEIN 1;1 (TIP1;1) at the vacuolar membrane¹⁶. In addition, while we restricted our analysis to a specific part of the root, it should be feasible to perform sptPALM in other epidermal tissues, such as for example young cotyledons and young leaves with a relatively thin cell wall, or hypocotyls (although the latter tends to have a high autofluorescence background in its cell wall). The feasibility of the approach in leaves is supported by the previously published sptPALM experiments in young *Nicotiana benthamiana* leaves^{19,20}. We can speculate that sptPALM should be feasible in protoplasts, but the difficulty might be for these protoplasts to remain stable over time, which might be achieved in microfluidic chambers or through confinement in micro-welled arrays⁴⁷. In addition, our analysis pipeline is not specific for plants and may be used to process sptPALM data acquired from other cells or organisms.

Comparison of sptPALM with other optical microscopy methods used to estimate diffusion

Comparison of sptPALM with other single molecule tracking methods. A number of alternative methods to sptPALM have been developed for single molecule tracking. Most of these methods rely on labeling the protein or lipid of interest with a fluorescent organic dye, such as HaloTag technology⁴⁸ or quantum dots. These labeling strategies have been successfully used in eukaryotic cultured model systems^{45,49-51}, bacteria⁵² and brain tissues^{53,54}. In contrast to sptPALM experiments, the use of bright and stable organic dye/quantum dots allows for tracking single molecules over a much longer period of time (typically >10/20 s, but can be variable depending on the imaging conditions). This increase in tracking duration is highly beneficial when dealing with molecules that have switching diffusion behaviors, as this is possible to analyze transition states on long tracks or to estimate dwell time at the plasma membrane^{55,56} or for protein-DNA interactions⁴⁹.

However, tracking with these labeling strategies requires a tight control of the density of labeled proteins/lipids to reach optimum single molecule imaging conditions. This is usually done by using low concentration of tags or using organic dyes with photo-physical properties compatible with single molecule conditions (such as TMR). Alternative solutions have also been proposed to control the density of emitters, for instance by designing stochastic labeling strategy based on translational readthrough error⁵⁷ or by designing new photo-activable organic dyes⁵⁸. Overall, these techniques deliver high-quality trajectories (in term of length) but they also record much less tracks than sptPALM, which can limit their statistical power.

In addition, in order to use proteins with small fluorescent labeled dyes, one depends on the external addition of either the labeled proteins (e.g. exogenous treatment with fluorescent

peptides), the dye (e.g. for HALO- or SNAP-tagged proteins) or antibodies⁵¹. The development of this labeling strategy has largely been hindered in plants because of the presence of the cell wall, which blocks or limits the delivery of the labeling system. However, covalent labeling of proteins using SNAP-tag and exogenous dye application was recently reported in the BY-2 culture cell system⁵⁹. In any case, one clear advantage of sptPALM is that the proteins of interest are labeled by genetically encoded FPs, which by-passes the need for external application.

Comparison of sptPALM with FRAP. FRAP can generally measure molecular diffusion in the range of 0.2 to 50 $\mu\text{m}^2/\text{s}$ ^{60,61}, while sptPALM is optimal in the range of 0.001 to 1 $\mu\text{m}^2/\text{s}$ (**Fig. 2**). FRAP is not a single-molecule imaging method but instead measures protein dynamics by averaging over the behavior of ensembles of biomolecules¹. It can thus be more difficult to extract biologically meaningful data when there are several subpopulations of molecules with different diffusion behavior (see phosphatidylserine sensor for example¹⁴). Indeed, FRAP analyses require choosing a model for data fitting, which can be complex when subpopulations of molecules exist. However, FRAP experiments also have some advantages. It can be performed with conventional monomeric FPs. Thus, it may be used on most transgenic lines currently available to study protein localization with fluorescent proteins, while sptPALM requires the specific design of reporter lines, which is time-consuming. In addition, FRAP is relatively easy to implement and can be performed on most microscopes, which facilitates its use.

Comparison of sptPALM with FCS. FCS measures the spontaneous fluctuations of fluorescence in an open volume defined by a focused laser and confocal optics⁶². Like FRAP, it can be used with conventional monomeric FPs, however, it requires specific dedicated equipment. FCS has a good temporal resolution (typically 10^{-2} to 10^2 $\mu\text{m}^2/\text{s}$, **Fig. 2**), making it particularly suitable for objects with a high diffusion coefficient. Indeed, those are hard to resolve by sptPALM even using stroboscopic illumination, because of camera speed limitations (with an upper bound <100Hz). However, a new tracking modality, called single-molecule displacement/diffusivity mapping (SMdM), can measure the instantaneous displacements of freely diffusing single molecules through the use of local statistics (**Fig. 2**)⁶³. Spatial information of diffusion related to membrane confinement or cytoskeleton corralling can also be retrieved from FCS measurement

by using variable observation volume^{62,64}. However, FCS is still limited to a small portion of the membrane and, as it is intrinsically based on fluctuations of fluorescence, it has difficulty to properly assess molecules with very confined diffusion⁶⁵. These aspects could constitute limiting factors for plasma membrane proteins in plants, which tend to have slow diffusion^{2,13,66}.

Dynamics vs. localization. FRAP and/or FCS techniques may be used as independent approaches to confirm and complement sptPALM experiments, as we did in our study on ROP6 dynamics in response to auxin¹⁴. It is worth mentioning that sptPALM experiments will not only provide diffusion coefficient, but also the super-resolved localizations of single molecules²², which are not provided by FRAP or FCS analyses and therefore add another layer of complementary information to diffusion measurements. Finally, a noticeable advantage of sptPALM, when performed in plant cells, is the ability to specifically analyze the membrane protein fractions and discard the cytosolic protein pool: plant cells have a high cytosolic streaming, which makes the diffusion of free cytosolic proteins too fast to be detected by the tracking algorithm and is therefore invisible by sptPALM. In the case of peripheral proteins, which associate transiently to the membrane, this allows focusing the analysis only on the membrane-bound fraction of the molecule.

Limitations of the protocol

This protocol can be implemented by a competent graduate student or postdoc trained in epifluorescence/TIRF microscopy and image analysis. As sptPALM is prone to detection artefacts, we strongly encourage setting up environmental conditions, such as controlled air or medium temperature, exposure to light during sample preparation and limiting mechanical stresses while handling the samples, to decrease background and to obtain reproducible experiments. Preliminary experiments should be performed with robust control lines and markers of interest to determine their basal state behavior before attempting treatments.

The sptPALM protocol described here has a number of limitations. First, it is only possible to measure protein diffusion in the membrane that is facing the coverslip, which restricts the

analyses to the epidermis and a single pole of the cell (outer later pole). Second, it is dependent on photo-activatable/switchable FPs. This limits the use of the this protocol to few transgenic lines specifically designed for sptPALM analyses. Indeed, most available transgenic Arabidopsis lines are made of fusion with classical FPs not activatable/switchable FPs. Preparing new transgenic lines stably expressing fusion with activatable/switchable FPs takes a significant amount of time (~6 to 12 months in Arabidopsis) and increases the risk that the expression of such fusion will not be suitable for imaging (e.g. low expression, unstable fusion, silencing of the construct, ...). Third, it is currently restricted to single color analyses — however could be extended to multicolor analysis in the future. Fourth, for a typical sptPALM experiment, thousands of individual tracks are recorded in a few minutes and analyzed in order to assess the diffusion properties of the protein of interest within the cell^{14,22,67}. Due to the lower brightness and photo-stability of FPs (as compared to organic dyes), the tracks are often very short in sptPALM, limiting the analysis of protein diffusion on longer time-scale (usually <1s). Thus, sptPALM is often not suitable to evaluate the dwell time of proteins at the plasma membrane or proteins with switching diffusion behaviors. Fifth, it is optimal to measure protein diffusion in the range of 0.001 to 1 $\mu\text{m}^2/\text{s}$, and hence is not suitable for faster moving soluble proteins.

Experimental design

Genetic considerations. The main constraint of PALM-derivative techniques is that they rely on photo-activatable or photo-convertible biomolecules. We routinely use fusion proteins with mEos2 as a photo-convertible FP¹⁴⁻¹⁶. mEos2 is one of the brightest photo-activatable/convertible FPs⁶⁸, yet it tends to be fainter than GFP/YFP derivatives when expressed in plant cells. Once transgenic plants are established, fluorescence should be checked using TIRF microscopy, rather than confocal microscopy, which is not as sensitive as TIRF microscopy. For example, we have

seen cases in which extremely low mEos2 signals could be detected in the green channel by confocal microscopy, while the expression level was suitable for imaging by TIRF after photo-conversion in the red channel. New mEos variants have recently been introduced, including mEos3.2, which is a true monomeric fluorescent protein⁶⁹, and mEos4.B, which has a better photostability and resists better to chemical preservation (i.e. cell or tissue fixation)⁷⁰. These new variants may improve sptPALM experiments, notably to obtain longer tracks, but they have not been tested in plant samples yet. It is important to note that mEos2 (and related FPs), occupies two color channels, which largely precludes its simultaneous use with additional genetically encoded fluorescent proteins for multi-color analyses. If two color analyses are required, researchers should consider using photo-activated (PA) FPs that use a single channel. For example, PA-GFP was successfully used in plants^{12,13} and thus could be used in the green channel. Red photo-activatable FPs, such as PA-mCHERRY, PA-mKATE, PA-tagRFP or PA-mRUBY3⁷¹⁻⁷⁴ exist, but, to our knowledge, have not been used so far for single particle experiments in plants and will have to be tested individually.

If possible, it is best to test the functionality of the fusion protein by checking its ability to complement the phenotype(s) of the corresponding loss-of-function mutant plants. We also advise to express the fusion protein under the control of its own endogenous promoter to obtain an expression pattern and expression level close to the endogenous protein. However, proteins with low expression levels in the root epidermis will not be optimal candidates for sptPALM analyses; if there are too few molecules to be imaged, this can bias the analysis because of a low sample size and/or increased background. If different experimental treatments or conditions will be tested, it is advisable to perform sptPALM on a set of control proteins that do not respond to the treatment. For example, we have used Lti6b-mEos2 as a fast-diffusible transmembrane protein and mEos2-AHA2/PIP2;1-mEos2 as a slow diffusing/immobile transmembrane protein¹⁵. These benchmarked fusion proteins and transgenic lines could serve as controls in future experimental set-ups.

Sample preparation. sptPALM experiments are extremely sensitive to micro-environmental factors because they follow the dynamics of individual molecules. Indeed, the dynamics of membrane proteins can be affected by external factors such as, for example, fluctuation in air or

medium temperature, changes of the orientation of the samples with regards to gravity, movement of the samples, mechanical stresses or light conditions. It is therefore of utmost importance to always handle plant samples in a controlled/reproducible way. We typically use dissected root from 5- to 12-day-old *Arabidopsis* seedlings and always incubate each root for 20 minutes in 3 ml control medium in a 12-well plate (without shaking), before performing the experimental treatment (for example with auxin, or DMSO for the mock treatment) for the desired amount of time. The roots are then directly mounted on the coverslip. To prevent sample squeezing, double sided tape can be used to create a space between the slide and the coverslip. Evaporation of the mounting liquid, due to long acquisition time, can be limited by sealing with lanolin/vaseline/paraffin (V/V/V) mixture. Dust and debris can be auto-fluorescent; it is thus crucial to be as clean as possible. Always use filtered buffer, single-use plasticware and cleaned coverslips and tweezers. It is of importance to always compare the obtained signal with the one from a mock-treated control. Consequently, this type of control experiment is mandatory for every treatment performed (as the treatment itself may induce an increase in autofluorescence). Be careful with solvents like DMSO or EtOH; depending on the concentration, they may have a strong impact on the dynamics of plasma membrane components. For example, auxin may be diluted in either DMSO or EtOH but we found a much higher impact of EtOH than DMSO on ROP6 diffusion. In any case, always dissolve the compound in the highest possible concentration of solvent (to reduce the amount of solvent used during the treatment) and perform control experiments with solvent only.

Choice of microscope and considerations for image acquisition. sptPALM experiment may be performed on any microscope with a TIRF set-up and equipped with a camera suitable for single molecule detection and allowing acquisition rate $>20\text{Hz}$. For highly diffusive proteins, it can be necessary to increase the acquisition frequency $>50\text{Hz}$ to avoid deformation of the point spread function (PSF). For regular emCCD cameras, it is usually possible to go beyond the limit of 30Hz by defining smaller ROI instead of working in full-frame mode. We have used the Zeiss Elyra PS1 system equipped with a $100\times$ Plan-Apochromat objective (NA 1.46) and an EMCCD (Andor iXonEM+)¹⁴, with a pixel size of $0.107\mu\text{m}$ and an exposure time of 20 ms. This last parameter being dependent on the camera framerate and protein diffusion. We typically image root epidermal cells from the elongation zone up to the fully differentiated cells^{14,15}, taking one

or two acquisitions per root tip (i.e. 3-6 cells). Only the fully expended root hairs are difficult to image since they are either too far from the coverslip or squeezed.

To discriminate between signal and background particular attention must be paid to the size and shape of the observable objects. Dust particles will appear as small immobile particles (2-3 pixels in diameter, below $0,1\mu\text{m}^2$) whereas mEOS2 emitting molecules will rather be around 5-6 pixels in diameter. Moreover, dust particles and mEOS2 particles can be discriminated by the fact that the density of photoconverted mEOS2 is proportional to the UV intensity, whereas the background fluorescence should remain constant. Finally, unlike mEOS2, background fluorescent particles are largely resistant to photobleaching and therefore are present all along the acquisition time resulting in long tracks.

Image analysis - Detection and reconnection. Once the data are acquired, the subpixel localization of each molecule has to be retrieved from its diffraction-limited image. The estimated position is then connected to the one obtained from the previous frame and the process is repeated until the trajectory of the molecule is fully reconstructed.

Many software are available to evaluate single-molecule localization from single-molecule localization microscopy techniques, but most of them do not propose a track reconstruction module⁷⁵. Only a few solutions combine track reconstruction and molecule localization. Among them, we historically used MTT (which is Matlab-based)^{45,46} for our sptPALM analyses^{14,15}. More recently, the open-source software TrackMate⁷⁶ was proposed and is a very good alternative for sptPALM analysis. TrackMate is indeed faster, easier to use due to a minimum number of parameters and runs under ImageJ/FIJI^{77,78}. Since both tracking solutions provide similar results, they have been implemented in our analysis pipeline and we indicate how to use either solution throughout the protocol. Because TrackMate is a fully open source freeware running with ImageJ/FIJI, we now favor this solution. For both software, single-molecule trajectories are reconstructed following a three-stage workflow: 1) detection of peaks potentially associated with single fluorescent emitters, 2) quality test and estimation of the subpixel position and 3) track reconnection.

For the detection/localization stage, we adjust the parameters in order to detect most of the single-molecule events present in the images while avoiding false-positive detections from the background. For MTT and TrackMate, two parameters need to be tuned:

- the size of the object we want to detect
- the detection threshold.

To help us optimize these parameters, both software provide built-in tools to overlay the detections with the raw images.

For track reconnection, both MTT and TrackMate ask for minimal hypotheses on molecule diffusion. In the case of plant membrane proteins that classically display an instantaneous diffusion coefficient between 0.001 and 1 $\mu\text{m}^2/\text{s}$, we have fine-tuned the reconnection parameters to work over this wide range of values (see Step 38-44 of the Procedure and Table 2). That way, each set of data is analyzed similarly, independently of the expected diffusion behavior of the proteins. Additionally, it is possible to set a blinking probability that allows a certain number of frames with missing detections within the same track. This is often needed to get long-enough tracks for the analysis.

The definition of the track reconnection parameters will require special care. Indeed, for many reasons, such as variation in fluorescent intensity, loss of focus or molecule blinking/photobleaching, an object detected at frame n can be absent at frame $n+1$. This can cause the premature stop of tracks. Oppositely, a newly activated fluorescent protein can also be confused with a recently extinct one. As a consequence, the tracks of two independent molecules would be fused with one another, appearing during the analysis as a unique track. This type of reconnection error is tightly linked to the density of molecules in the sample and could be controlled experimentally by modulating the fluorescent proteins activation (see the previous section “Choice of microscope and considerations for image acquisition” and Step 22 of the Procedure).

To assess the quality of the reconnection, we use a home-made graphic user interface called sptPALM_viewer (<https://github.com/jbfiche/sptPALM>). This interface is used to calculate the MSD and apparent diffusion coefficients of the tracks output by MTT/TrackMate (see the

following section “Image analysis - Calculation of the mean square displacement and instantaneous diffusion”). It also allows to check each track one by one for some benchmarked experiments. In addition, sptPALM_viewer can generate a cumulative distribution of particle step length in order to define a maximum distance between two consecutive detections. This correction usually suppresses most of the reconnection errors. As a final verification, a visual inspection of the tracks can be performed on a reconstituted image, where all the tracks from a movie are represented. Note that our sptPALM_viewer may also be used to analyze single particle tracking experiments recorded by other microscopy modalities (confocal microscopy, structured illumination microscopy, or light sheet fluorescence microscopy), but in this case, it will not track single molecules.

To fine-tune the MTT/TrackMate and sptPALM_viewer parameters, it is important to run some controls. Plants expressing proteins with a well-described diffusion behavior can be used for benchmarking⁶⁶ (see Experimental Design – Sample Preparation). Additionally, it is possible to measure the diffusion of fluorescent beads in controlled environments such as water/glycerol mixtures⁷⁹. In that case, knowing the experimental conditions (radius of the fluorescent beads, temperature and dynamic viscosity of the medium — http://www.met.reading.ac.uk/~sws04cdw/viscosity_calc.html), it is possible to theoretically derive the diffusion coefficient based on the Stokes-Einstein equation and to compare it with the results of sptPALM measurements. Finally, simulated data can be used to test the robustness of selected parameters in the case of extreme diffusion behavior or mixed populations. To this end, we have added a simulation module to sptPALM_viewer.

Image analysis - Calculation of the mean square displacement and instantaneous diffusion.

One of the most common approaches to quantify molecular diffusion is by calculating the mean square displacement (MSD), which is defined as:

$$MSD \equiv \langle |x_t - x_0|^2 \rangle$$

It measures the deviation of a diffusing object over time at position x_t with respect to a reference position x_0 . In practice the MSD is calculated for each track using the following definition:

$$MSD_n = \frac{1}{N-n} \sum_{i=1}^{N-n} (\mathbf{r}_{i+n} - \mathbf{r}_i)^2, n = 1, 2, \dots, N-1$$

where N is the total number of detections in the track and \mathbf{r}_i is the i^{th} position within the track. The MSD is calculated based on all available displacements ($N-n$) of a given duration $n \times \Delta t$, the value of Δt indicating the duration between two consecutive images. From this expression, we understand that the MSD values will be properly averaged only for the smallest values of n .

It is worth noticing that the MSD is not the only method allowing an estimation of the diffusion coefficient. In particular, analysis based on step length distribution is also used^{63,80,81} though it is more suited for highly dynamic diffusion and/or very short tracks.

The shape of the MSD curve informs about the type of diffusion the protein is undergoing⁸². Brownian motion diffusion in isotropic medium presents a MSD curve that is linear over time, with the following expression for 2D diffusion^{83,84}:

$$MSD(t) = \epsilon + 4Dt$$

According to this equation, the diffusion coefficient D of the protein can be directly estimated based on a linear fit of the MSD curve.

In the case of non-Brownian diffusion, the MSD curves will quickly diverge from this simple linear behavior. In particular, for constraint diffusion, the MSD will plateau with an asymptotic value related to the geometry and confinement size L_c of the molecules^{82,83}. However, as long as $t \ll L_c^2/D$, the linear behavior of the MSD is a fairly good approximation and it is possible to infer the instantaneous diffusion coefficient (D_{inst}) assuming Brownian diffusion within the confinement zone.

The MSD is calculated based on the estimated localizations of the diffusing molecule, resulting in two types of uncertainties influencing its calculation⁸⁴. First the precision of localization σ ⁸⁵ which depends strongly on the brightness of the emitter, the quality of the detector and the intensity of the background in the sample (background signal being a true signal that originates

from within the specimen, e.g. due to autofluorescence) and the acquisition noise (noise being created by the detection system, e.g. by random electrical discharge of individual pixels within the camera chip). On the other hand, for fast diffusion, the emitter can travel distances larger than the diffraction limit during the exposure time t_e , leading to deformation of the PSF and eventually preventing proper localization by the detection algorithm. The reduced localization error x can be computed in order to estimate which of the two sources of error is predominant:

$$x = \frac{\sigma^2}{Dt_e}$$

For $x \gg 1$, the localization error is the main source of error, the distance travelled by the molecule being small as compared to the uncertainty on the emitter position. Interestingly, in this regime, the intercept ϵ of the linear regression of the MSD over time is a direct measurement of the localization precision:

$$\epsilon \simeq 4\sigma^2$$

On the other hand, for $x \ll 1$, the uncertainty on the emitter localization is completely dominated by diffusion. It is however important to note that, for our sptPALM experiments, we carefully optimize the exposure time t_e in order to avoid any observable deformation of the PSF due to diffusion, while ensuring enough intensity for the detection.

To achieve accurate MSD estimation, it is essential to pre-process the data and to select only tracks of good quality. Three parameters can be tuned in the sptPALM_viewer software. First, only tracks that are at least 7 frames long are considered. Due to blinking/missing detections/out-of-focus motion, the tracks are not necessarily complete and the location of the emitter can be missing for several time points. Therefore, a second parameter is defining the maximum number of frames separating two detections (by default this parameter is set to 3 frames). And finally, a third parameter is checking that each track is at least 75% complete. A direct consequence of these filters is the loss of more than half of the recorded tracks. Indeed, due to the photophysics of mEos2 (e.g. fast blinking with short ON time and long OFF time, photobleaching, etc.), a large number of the tracks are less than 7 frames long.

As stated before, D_{inst} can be estimated using a linear regression of the MSD curve. For the reasons stated before (small track length, error on the MSD estimation, non-Brownian behavior, etc.) the MSD will have a linear behavior only for the lowest values of $n \times \Delta t$ and the regression will be limited to the first points of the curve. By default, we use the first four points for the regression but this parameter can be adapted according to the diffusion properties of the protein under study⁸⁴.

Considering previous published works, both theoretical and experimental^{16,84}, our experimental conditions are optimal for a diffusion range from 0.1 to 0.01 $\mu\text{m}^2/\text{s}$. For diffusion coefficients above 0.5 $\mu\text{m}^2/\text{s}$, the exposure time and the excitation laser power would have to be optimized in order to avoid PSF deformation and mislocalization errors. Indeed, the molecules can cross distances higher than the diffraction limit if the exposure time is too long, leading to aberrant PSF shapes that could eventually be excluded during the detection step. Moreover, the probability of reconnection errors will increase as tracked objects will explore more space between two consecutive frames.

To experimentally determine these upper limits for D_{inst} , plants expressing fast diffusing protein can be used. For instance, TIP1;1 (a tonoplast localized aquaporin) was reported to have a D_{inst} around 1 $\mu\text{m}^2/\text{s}$, which is usually way higher than plasma membrane-localized proteins¹⁶.

Similarly, for very low diffusion coefficients ($<0.01 \mu\text{m}^2/\text{s}$), uncertainty on the emitter localization dominates the precision of D_{inst} estimation. Indeed, due to camera noise and low signal-to-background ratio, single mEos2 molecule localization precision is usually around 30 nm in our conditions. Using recombinant purified mEos2 proteins immobilized on a coverslip surface we found the experimental lower bound of D_{inst} to be equal to 0.001 $\mu\text{m}^2/\text{s}$.

Finally, our sptPALM_viewer is implemented with a simulation module that can help optimize the set of parameters used for the detection (MTT or TrackMate) and the analysis (sptPALM_viewer). One or two sub-population(s) of particles can be simulated with different diffusion coefficient values and ratio. Videos can be generated with stochastic appearance of particles with predetermined ON and OFF state, blinking behavior, and signal-to-noise ratio. The

parameters of the emCCD detector and the imaging conditions can also be tuned according to the typical experimental conditions. The simulated movies can then be analyzed in order to test whether we can retrieve the diffusion properties of the simulated sub-populations.

Statistical analysis. For each tested experimental condition, after a first interactive exploration (see Steps 56-62 of the Procedure), we aim at statistically validating the existence of one or two sub-population(s) of molecules, which is more or less apparent from their $\log_{10}(D_{\text{inst}})$ values (see Steps 63-66 of the Procedure). For that purpose, we rely on the Mixture Modeling (MM) framework as a data-driven partitioning of immobile/slow and mobile/fast molecules. We first propose the use of Gaussian MM (GMM⁸⁶) using the *mclust* R package as in¹⁴. Briefly, 3 GMMs are competed with either $G=1$ or $G=2$ Gaussian components. The parameters of the GMM - a mean μ_g , a variance σ_g^2 and a mixing proportion p_g of each g^{th} Gaussian component(s) ($p_g > 0$, $p_1 + p_2 = 1$) are estimated by maximization of the likelihood with a modified Expectation-Maximization (EM) algorithm^{86,87}. The mixing proportions p_g can be viewed as a prior probability that any track belongs to the g^{th} component. Two components can be constrained to share the same variance ($\sigma_1^2 = \sigma_2^2 = \sigma$), denoted by the “E” model, or have variance-specific ($\sigma_1^2 \neq \sigma_2^2$) value, denoted by the “V” model. We use a likelihood-based criterion, the Bayesian Information Criterion (BIC), to retain the best model, i.e. with the smallest BIC value. All $\log_{10}(D_{\text{inst}})$ values per cell are pooled and if one Gaussian is retained, there is no threshold to be set, otherwise an optimal threshold is set according to the Maximum A Posteriori (MAP) rule where every single track is assigned to the component corresponding to the highest component membership posterior probability. The threshold corresponds to the intersection point of the two posterior probabilities of belonging to each component. Tracks with $\log_{10}(D_{\text{inst}})$ values below this threshold refers to the slow sub-population, whereas values above denote the fast sub-population. Finally, a 95% confidence interval (CI) is reported by default for each estimated parameter of the GMM by bootstrapping, using 999 bootstrap replications.

It is important to note that GMM assumes the presence of symmetric components although empirical data may be more complex, with presence of asymmetry in one component. We therefore additionally propose to extend the Gaussian case by allowing the presence of skewness, determined by one additional shape parameter⁸⁸. Each component g of such mixture of scale

mixtures of skew-normal (denoted as FMSMSN⁸⁹) is thus characterized by a location ϵ_g , a scale λ_g^2 , a shape β_g and a mixing proportion p_g . The mean and variance of each component can be found back by $\mu_g = \epsilon_g + \lambda_g \delta_g \sqrt{(2_g/\pi)}$ and $\sigma_g^2 = \lambda_g^2 (1 - 2 \delta_g^2/\pi)$ with $\delta_g = \beta_g/\sqrt{(1+\beta_g^2)}$. The principle is the same as for the GMM except that 95% (default) CIs are obtained using the Fisher information matrix. From this analysis, several graphs and tab-separated text files are generated in order to perform further statistical analyses or data visualization.

Materials

Biological Materials

- Arabidopsis thaliana transgenic seeds expressing the protein of interest fused with Photo-Activable (PA-GFP, PA-mKate PA-mCH) or photo-convertible (mEos2) fluorescent proteins. Transgenic marker lines expressing fluorescent fusion proteins were used for control: WT Col0 (NASC #1092), *35S::mEos2-PH^{EVECT2}* phosphatidylserine biosensor¹⁴, *PIP2;1-mEos2⁶⁶* and small integral plasma membrane protein *LTI6b-mEos2¹⁵*.

Reagents

- MilliQ water, >18MΩ·cm, 0.22 μm filtered, Ultrapure water (Dutscher 069802A)
- Murashige and Skoog (MS) Basal Salt mixture (Sigma-Aldrich, M5524)
- Plant Agar (Duchefa P1001)
- Acetone (VWR 20063)
- Ethanol ≥ 96% (VWR 83804)
- 8M KOH stock solution (Sigma-Aldrich P4494)
- Lanolin (Sigma-Aldrich L7387)
- Vaseline (Sigma-Aldrich 16415)

- Parafin (Sigma-Aldrich 327204)

Equipment

- Jar & Rack Staining jar 50 slides (Dutscher 048903), plastic rack (VWR 631-9520)
- Coverslips Menzel glaser 24×40 mm (VWR, MENZBB024040M113), 0.13 – 0.16 mm thickness
- Microscope Slides (Sigma-Aldrich CLS294875X25)
- Corning® Costar® TC-Treated Multiple Well Plates size 12 wells (Sigma-Aldrich CLS3513-50EA)
- lens cleaning tissue (Thor labs, MC-5)
- Surgical tape 12.5mm (VWR, 115-8172)
- 0.22 µm filters (Merck SLGS033SS)
- Square Petri dishes (Dutscher 132511)
- Aluminum foil (Sigma-Aldrich Z185140)
- Razor blades (Dutscher 132511)
- Tweezers Dumont #5 (Fischer, 15483542)
- Microscope equipped with a TIRF arm and a TIRF objective (for examples, Zeiss Elyra 7, Gataca Systems Ilas3 module, Leica DMI8 S module infinity TIRF, ...)
- Ultrasensitive EMCCD camera dedicated to single molecule detection (for example, Andor iXonEM+ or XU_897)
- A computer with at least 8 GB of RAM, a SSD disk with >100GB, multi-core processor

Software

- ImageJ/FIJI (<https://fiji.sc/>)
- MATLAB runtime for R2019a, standalone set of shared libraries that enable the execution of compiled MATLAB applications or components (https://www.mathworks.com/products/compiler/matlab-runtime.html?s_tid=srchtitle)
- sptPALM_viewer code is available on GitHub (https://github.com/jbfiche/sptPALM_cbs) and a standalone application is freely available here (http://bioserv.cbs.cnrs.fr/DOWNLOAD/sptPALM_data/ in the Softwares.zip file)

- MTT (<http://www.ciml.univ-mrs.fr/fr/technologie/imagimm/software>)^{45,46} or TrackMate (<https://imagej.net/TrackMate>)⁷⁶
- Stack_Split_macro.ijm (http://bioserv.cbs.cnrs.fr/DOWNLOAD/sptPALM_data/ in the Softwares.zip file)
- SPTpalm_Rscript.R R script (http://bioserv.cbs.cnrs.fr/DOWNLOAD/sptPALM_data/ in the Softwares.zip file)
- RStudio software (<https://rstudio.com/products/rstudio/download/>; using R version 4.0.0) to open and run the “SPTpalm_Rscript.R” script
- data.table (<https://cran.r-project.org/web/packages/data.table/index.html>; version 1.12.8)⁹⁰, mclust (<https://cran.r-project.org/web/packages/mclust/index.html>; version 5.4.6)⁹¹, mixsmsn (<https://cran.r-project.org/web/packages/mixsmsn/index.html>; version 1.1-7)⁸⁹ R packages. These packages can be easily installed from the RStudio terminal using the `install.packages("package_name")` command.

Reagent Setup

MS Solid medium: Prepare MS basal salt mixture by combining MS Basal Salt mixture (4.33 g/L) and 0.8% (wt/vol) agar. Adjust the pH to 5.7 with 0.1M KOH. Sterilize the MS medium by autoclaving and cool the medium before pouring the plates.

MS liquid medium: Prepare the MS liquid medium by combining MS Basal Salt mixture (4.33 g/L). Adjust the pH to 5.7 with 0.1M KOH. Sterilize the MS liquid medium by autoclaving and filter using a 0.22 µm filter. and the MS liquid medium can be stored at room temperature and should be used within two weeks

Procedure

Sample preparation. Timing 1 hour + 5 days for plant growing

1) **Coverslip cleaning (Steps 1-8):** Transfer the coverslips on the stainless-steel/plastic rack and place it in the staining jar (**Fig. 3a and b**).

Critical step: Proper cleaning of coverslips is a crucial step to avoid dust, unspecific detections and background fluorescence.

2) Add 100% acetone in the jar and incubate 10 minutes under a chemical hood.

3) Remove the acetone and replace by 96 % EtOH, incubate 5 minutes. Replace the EtOH by fresh 96% EtOH and incubate for another 5 minutes.

4) Remove EtOH and replace by MilliQ H₂O containing 1M KOH, incubate 10 minutes.

5) Rinse five times with milliQ H₂O (without KOH).

6) Remove the rack from the jar and place it on paper tissue to remove the excess of water.

7) Carefully set up a Bunsen burner flame. Close the collar (air regulator), then turn the collar back to let a small amount of air pass through. Open the gas tap and generate sparks over the Bunsen burner. The flame should have a yellow/orange color. Increase the flame heat by turning the collar until the flame turns blue. The temperature is critical because if it is too low it will result in black residue on the coverslips and if it is too hot the flame will damage the coverslips.

8) Carefully remove one by one the coverslips from the rack using clean tweezers, flame dried them for approximately 10 seconds by passing through the flame on one side then the other. Once there is no more water, put the coverslips in culture plates, which have been covered with aluminum foil beforehand.

? TROUBLESHOOTING

Critical step: Trash coverslips that have rifts, bends or visible residues.

PAUSE POINT. Once wrapped in aluminum foil, the cleaned coverslip can be stored for several months.

9) **Plant culture (Step 9).** Grow *Arabidopsis* seedlings vertically on solid MS medium for 5 days in square Petri dishes.

Critical step: Plant lines expressing tagged proteins with known dynamics at the plasma membrane should be used as controls. We routinely use LTI6b-mEos2 and PIP2;1-mEos2¹⁵ as examples of highly mobile and immobile proteins at the plasma membrane, respectively. In addition, the phosphatidylserine biosensor mEos2-

PH^{EVECT2} can be used; this protein is present in two states (mobile/immobile) at the plasma membrane¹⁴.

10) **Sample preparation (Steps 10-13):** Carefully dissect roots 1.5-2 cm from the root tip and transfer them in 12-well plates supplemented with 3 ml medium (classically liquid MS medium without sugar) using tweezers. Alternatively, the entire seedlings can be transferred to the well (**Fig. 3c**).

Critical step: To ensure proper treatment and homogenous results ensure that specimens are fully immersed in the medium.

11) Incubate 20 min without shaking before transferring the roots into a new well containing the desired treatment (hormone for example) (**Fig. 3c**).

Critical step: Take along the required controls and mock treatments. Use a new well for each treatment. Properly clean tweezers between every sample transfer to avoid control or mock medium contaminations with treatment medium.

12) Place a cleaned coverslip on a lens cleaning tissue immobilized on the bench using surgical tape, add 60 µl of mounting medium (liquid MS medium) onto the coverslip. If the coverslip is perfectly clean, the medium droplet should spread over the surface (**Fig. 3d**).

13) Place the roots in the middle of the coverslip, perpendicularly to its main axis (**Fig. 3e**). Carefully place the microscope slide on top of the sample (be careful to not crush the samples). Proper cleaning of coverslips should prevent the formation of air bubbles between the two glass layers. Tape both sides of the coverslip to the slide to ensure proper assembly and spacing (**Fig. 3e and f**). A spacer of 2 to 3 layers of tape can be added both sides in between slide and coverslip to prevent sample crushing.

Critical step: Avoid squashing the sample as it will affect protein dynamics at the plasma membrane. Moreover, damaged cells will release fluorescent proteins in the medium creating false-positive detections everywhere. Sample integrity has to be checked using transmitted light. Further controls to ensure the integrity of the sample must be done during the acquisition steps, see below.

Image acquisition (TIMING 4 hours)

- 14) ***Setting the microscope parameters (Steps 14-25)*** Place the sample under the microscope. In our example, imaging is performed on a Zeiss Elyra PS1 system with a 100 \times Plan-Apochromat objective (NA 1.46), in TIRF mode (TIRF angle between 63 $^{\circ}$ and 73 $^{\circ}$).

Critical step: Always image WT non-transgenic lines using the same illumination conditions as with fluorescent samples to ensure that medium and coverslips are clean (no or very few fluorescent event(s) should be detected).

- 15) Specify the imaging parameters in the ZEN software. To maximize the signal-to-noise ratio, set gain parameter to 300. The pixel size was 0.107 μm .
- 16) Name the collected Raw data “Construct_treatment”.
- 17) Saved the collected Raw data in a single folder (Example Date/RawData).
- 18) Record 10,000 image time series at 50 frames per second (20 ms exposure time) on a 256 x 256-pixel Region Of Interest (ROI) (the size will depend on the readout of the camera). Using those experimental conditions, 3 minutes and around 20 seconds are required to acquire a single sptPALM experiment.

Critical step: We chose this duration for each time series because this is a good tradeoff between the maximization of the number of events recorded and the stress experienced by the plant. It is important to check if the imaging could influence the biological response under study. Typically, post-acquisition, it is possible to split the time series in smaller movies and analyze them separately in order to confirm the stability of the results over the course of the acquisition.

- 19) Activate the Zeiss Definite focus to ensure focus maintenance and set automatic re-adjustment every 2,000 frames.
- 20) Photo-convert mEos2 by continuously applying a 405-nm UV laser during the acquisition.
- 21) Excite photo-converted mEos2 using a 561-nm laser.
- 22) Adjust the UV laser power to photo-activate a significant number of molecules without having too many molecules activated at the same time to facilitate further analyses. Use between 0.01 and 0.1% of laser power usually for a Zeiss Elyra PS1, to 0.1 μW -1.03 μW at the objective.

Critical step. Empirically adjust the UV laser intensity to obtain between 10 and 25 molecules detection per frame. If the number of activated molecules is too low, they will be detected easily, but the number of tracks will be low, which will diminish the statistical power of the analysis. By contrast, if the number of activated molecules is too high, they will be hardly localized correctly, which will lead to errors in track reconstruction. It is therefore required to empirically adjust the laser power to reach an optimum balance between detecting enough molecules and being able to separate single activated molecules. **Fig. 4a** shows a typical example of an acquisition with only a few visible molecules due to a low number of photo-conversion events (the UV laser power is too low). In **Fig. 4b**, the 405-nm laser power was slightly increased to reach enough photo-conversions (between 10 and 25 molecules per frame, here 17 spots). **Fig. 4c** shows an example where the UV laser power was too high, resulting in too many detections. In that case, the high proximity of detected molecules might lead to errors in track reconstruction, see **Fig. 4d** magnification of **4c**.

? TROUBLESHOOTING

23) The 561-nm laser intensity will also influence the molecule density by impacting the life-time before mEos2 molecules photo-bleaching. Use between 10 and 20% of laser power usually for a Zeiss Elyra PS1, to 3.2 mW-6.35 mW at the objective.

Critical step: To ensure a proper localization of the fluorescent particles, the signal-to-background (S/B) ratio must be equal or higher than 4 in our setup (where background signal is true signal that originates from within the specimen, e.g. due to autofluorescence). Calculate the S/B ratio by opening a movie with ImageJ and draw a line across a spot using the line-tool. Measure the signal along the line using the “Analyze/Plot Profile” tool (**Fig. 4g and h**). The highest value of the resulting intensity curve will provide an estimation of the fluorescent signal of interest (Si). Estimate the background intensity by drawing a circular ROI of a few pixels in diameter (>10), close to the fluorescent spot to have comparable excitation intensity. No detection should be seen within this ROI and it must be inside the cell in order to

measure the influence of the cellular background fluorescence. Measure the fluorescence background (B) using the standard deviation of the signal.

- 24) Test the potential effect of the imaging on protein diffusion by comparing the first and the last 1,000 images of a single time series. If you observe large difference between the beginning and the end of the acquisition, discard the observation and set new imaging parameters (Steps 14 to 23). Parameters that can be adjusted include reducing laser power, the length of the acquisition or the laser incident angle.

? TROUBLESHOOTING

- 25) Repeat Steps 14 to 24 no more than three to four time on the 2-3 root tips before changing the slide.

- 26) *Assessing that you are working in single molecule conditions (Steps 26-28)*. Ensure that the fluorescence of single emitters disappears in a single-step transition. If the intensity of the emitters is gradually decreasing, it means that several emitters are detected within the same diffraction-limited volume.

- 27) Check that a single emitter goes under stochastic dark state (blinking) (**Extended Data Figure 1a and b**). This phenomenon is not visible if several molecules are activated within the same Airy disc. In practice, when setting up the experiment, measure the intensity of several emitters over time and check that photo-bleaching/blinking happens as a single-step transition.

- 28) For immobile/slowly diffusing proteins, perform intensity measurement using ImageJ/FIJI by selecting a small ROI around the emitter and apply the Image/Stack/ z profile tools in order to get the intensity variation over time.

- 29) *Checking for false-positive detections and background fluorescence (Steps 29-34)*:

Include in the field of acquisition an area without any cells. Make sure that no signal is seen in such area.

- 30) Perform a global visualization of the acquisition using ImageJ/FIJI Stack tool “Max Intensity” projection. A projection of 1,000 frames out of the 10,000 (**Fig. 4e**) will create a new image with maximum value for each pixel over time resulting in a

- projection of all spots. Check the signal in the regions between cells or out of the sample on such projection, they should show no or low signal.
- 31) Visualize the cellular background using the ImageJ/FIJI Stack tool “Median Intensity” projection. In **Fig. 4f**, the cell wall background appears as a diffuse signal whereas dust particles look like bright spots. Squashed samples will result in high background and detection outside expected membrane areas.
 - 32) If the S/B ratio is too low, increase the 561-nm excitation laser power (Step 23). However, keep in mind that high excitation power will increase the photo-bleaching rate of the fluorescent proteins and consequently, will reduce the average track length of your detections.
 - 33) Depending on the sample and its position with respect to the coverslip, optimize the signal-to-background ratio by carefully adjusting the laser incident angle in order to reach VAEM or TIRF illumination conditions (Step 14). If the incident angle is too small, fluorescence arising from intracellular compartments can be detected (rather than from the plasma membrane only) and degrade the signal-to-background ratio of the images. On the other hand, if the incident angle is too high, the excitation of the sample will no longer be optimum and no fluorescence signal will be detected.
 - 34) As already described in the literature⁹², sample illumination is often uneven when using laser excitation. To attenuate this phenomenon, use spinning azimuthal excitation, which results in a more homogeneous field of excitation^{92,93}.

PAUSE POINT. Once acquired, images can be analyzed at any time.

? TROUBLESHOOTING

Image analysis. TIMING 1 day

Critical Single-molecule detection and tracks reconstruction can be done with the MTT algorithm^{45,46}. Further computational analyses of tracks are carried out using sptPALM_viewer^{14,15}. Note that, as an alternative to MTT, molecules detection and reconnection can be achieved with TrackMate⁷⁶. Step 35 to 44 explains how to use the MTT software. For TrackMate, please refer to the TrackMate user manual⁷⁶ and go directly to step 45.

- 35) *Detection and reconnection (Steps 35-53)*: Split the time-lapse file of 10,000 images in ten stacks of 1,000 images each to facilitate the tracking analysis by MTT software (mainly computer memory management). Run the macro (Stack_Split_macro.ijm) to do this for .lsm files.
- 36) Select the “Source Directory” and then indicate the destination directory where the new stacks will be saved afterwards. Each new stack will be renamed “original_name”1, “original_name”2, “original_name”3, etc, up to “original_name”10 and saved in a directory named like the original file.
- 37) Organize the resulting data as followed:
Date/Analyses/Constructs/Treatment/AcquisitionNb.
- 38) Open the MTT software
- 39) Load load_MTT.exe and select “MTT with tracking (expert mode)” and “GO !!!!” (**Fig. 5a**).
- 40) Load the data by clicking on “Choose the image(s) to read”. All .tif files will be loaded even if they are located in subfolders.
- 41) Set the parameters for every section: “Detection Parameters”, “Validation of pre-detected particles” and “Reconnection Parameters” (See Table 1 for a description of the parameters) (**Fig. 5b**).
- 42) Select “.mat” as output file type.
- 43) Open a single image by clicking “Click here” to set up the “Alpha threshold” value (**Fig. 5c and d**). Choose the pixel value threshold, and click on “Go” to see particles detected above this value.
- 44) Once this parameter has been reliably fixed and all the particles are well detected, launch the analysis by clicking “Start the Analysis” (**Fig. 5b**). The output of MTT will be: one folder per stack named “original_name”.tif_output containing .mat file with all trajectories detected and a .txt file with all parameters summary.
- 45) Launch sptPALM_viewer to further analyze both the trajectories and localizations of the particles,. The display window will appear (**Fig. 6a**).
- 46) Fill the pixel size of your images and the lag time between two consecutive frames (as specified in Steps 15 and 18).

47) Select the type of data to upload depending on the type of detection and reconnection software (MTT or TrackMate). Click on the “Load MTT files” or “Load TrackMate files” button to load the tracks output files.

Critical step: By selecting a folder, the software will load all .mat/.xml files and calculate MSD, D_{inst} and $\log_{10}(D_{inst})$ on all datasets, allowing cell-per-cell analysis or pooling all cells with the same background and/or treatment. When ticking the “Save trajectories” option, two text files will be created. The first one will contain all the xy coordinates of the detected objects (“Localizations.txt”), whereas the second consists in track centroids and lengths of all trajectories (“Localizations_average.txt”). These data can be directly used for particle clustering analysis, using for instance the SR-Tesseler software^{14,15,94}. Loading tracks will generate two outputs: the cumulative distribution of the step length and the histogram of trajectories duration (**Fig. 6b and c**). These plots give an overview of the properties of the reconstructed tracks. In the statistics panel, the number of movies and the number of trajectories loaded will be indicated (**Fig. 6a**). Both plots are automatically saved in the folder.

? TROUBLESHOOTING

48) In case the selected files were previously loaded and analyzed, a .mat file containing the raw data as well as the results of the analysis is created. The name of this file can be modified in the “Saving file name” edit-line. When loading already analyzed MTT/Trackmate files, a dialog box will display the following message: “Previous analysis with the same name was found. Do you want to proceed anyway (previous data will be lost)?”. This message indicates that the data have been already analyzed and the .mat file containing the results of this analysis was found in the selected folder. Click “Load previous analysis” to load the result files and apply different filtering parameters on the tracks. Click “Proceed” for reloading the files and starting a new analysis.

49) Visualize the time-lapse stacks and corresponding trajectories using the visualization tool (**Fig. 6d**).

50) Click on “Load movie” to select a .tif file, then click on the “Load trajectories” button to select the associated .mat/.xml files in the corresponding folder.

- 51) Upon loading both files, adjust “Contrast (upper limit)” to see the signal.
- 52) Use the “Select frame” to select time points. Reconstructed trajectories will be added to the image, color-coded in blue for early time points of the tracks shifting to green and red for later time points (**Fig. 6d**).
- 53) Optional: Export the video as .avi.

54) **Analysis parameters panel (Step 54-55)**. Filter short tracks or tracks with missing points by adjusting the analysis parameters panel (see Table 2 for a full description).

Critical step: Parameters can be re-adjusted after a preliminary analysis that clearly shows aberrant reconnection (i.e. straight reconnection between two points above a certain distance). In these experiments, the following parameters were used: 0.75 μm as a maximum distance between two detections, no blinking was allowed (0), only tracks with at least 7 frames were selected, and 4 points were used for computing D_{inst} . The display time for MSD was set to 0.5s. Because soluble proteins (such as free mEos2 for example) diffuse rapidly, they travel a distance greater than 0.75 μm between two successive acquisitions and thus are not detected as tracks by the sptPALM_viewer software.

55) Adjust the blinking threshold to increase the number and the length of the tracks. We usually use values from 0 to 3 but it is necessary to verify the quality of the track reconnection.

Critical step: As explained before, the particle density can lead to some reconnection errors. They can be identified on the “Trajectories.png” file (Step 59), as they will appear as straight lines connecting two points above a certain distance (**Extended Data Figure 2a**). Another type of wrong trajectories corresponds to very long tracks that are likely due to background signals (**Extended Data Figure 2b**). See troubleshooting Table 3.

56) **MSD & Diffusion analysis: a viewer (Steps 56-62)**. Click on “Analyse trajectories”.

Critical step: sptPALM_viewer proposes two different ways to estimate molecule instantaneous diffusion based on MSD calculation. MSD curves are computed for each preselected track (see before). D_{inst} can be classically estimated by fitting a

linear regression on MSD versus time, over a predefined number of points.

Alternatively, sptPALM_viewer can retrieve D_{inst} estimate by directly calculating the ratio of the MSD over time: this method is less computationally demanding and can be used as a first approximation, it is also less accurate for D_{inst} below $0.01 \mu\text{m}^2/\text{s}$. Therefore the regression procedure should always be favored.

- 57) A dialog box will ask for Region Of Interest (ROI) selection. If desired, click Yes and select a movie from the same dataset as the .mat/.xml file. It will be used to calculate an average intensity image.
- 58) Draw an ROI to analyze a given cell from the field of view or to work on the background area. Note that the results will be saved in a .mat file with names indicated in “Saving file name” edit-field. Therefore, a specific name file can be saved for each ROI.

Critical step: As explained in the section “Calculation of the mean square displacement and instantaneous diffusion” the number of points selected for the linear fit is a critical parameter for the estimation of D_{inst} . By default, it is set to the first four points of the MSD curve but it can be optimized depending on the diffusion properties of the proteins under study. At the end of the processing, the user can manually explore heterogeneity within each cell for a given condition.

- 59) A dialog box will open with two options: “Do you want to fit the distribution with one or two Gaussian?”. Select the one-population option if your molecule of interest appears to behave homogeneously as a single population (and seems valid for example for Lti6b-mEos2 and PIP2;1-mEos2 lines, **Fig. 7a and d**). The output files will be as followed: histogram of $\log_{10}(D_{inst})$ (“Diffusion_distribution_Fit_Method.png”), values (“Saved_Diffusion_Coeff.txt”) (**Fig. 7a and d**), MSD plotted over time (“MSD_Curves.png”) and values (“Saved_MSD.txt”) (**Fig. 7b and e**). If the “Plot trajectories” option was ticked, the projections of all trajectories (“Trajectories.png”) will be plotted (**Fig. 7c and f**).
- 60) If two sub-populations of molecules are apparent (**Fig. 7g**), mouse click on the approximate separation between sub-populations. This will provide starting values to parameterize the two Gaussian distributions, each associated with one of the two sub-populations (“FitGaussianDistribution.m”). The two resulted Gaussian densities,

scaled to the proportion of molecules in each sub-population (mEos2-EVECT line **Fig. 7g and i**), will then be overlaid with the histogram of $\log_{10}(D_{\text{inst}})$ values. In the output files, the $\log_{10}(D_{\text{inst}})$ values will be partitioned between the fastest (orange, biggest mean) and the slowest (blue, smallest mean) sub-populations (**Fig. 7h**). The threshold value for the partitioning is defined by the intersection of the two Gaussian densities. In addition, two MSD curves will be calculated as a function of time and displayed according to the same color code (**Fig. 7i**). Note that each MSD curve corresponds to the median MSD over time calculated from all the tracks belonging to the selected cell.

? TROUBLESHOOTING

- 61) Select “Trajectories plot (two populations)” and “Plot previous analysis” to visualize the two sub-populations of trajectories (**Fig. 7j and k**). The trajectories will be color-coded with the tracks corresponding to fast diffusing molecule in orange and the tracks corresponding to slow diffusing molecule in blue (**Fig. 7k**). Note that a complete statistical analysis is available and detailed in the next section (“MSD & Diffusion analysis: a data-driven partitioning using Mixture Modeling” Steps 63-66) where the two Gaussians, denoted as a “mixture” of distributions, are estimated and tested on the pool of cells for a given condition. This will avoid that one cell gives a spurious idea of the behavior of all cells under this condition. Note that all output files are automatically saved in the folder.
- 62) Retrieve additional information in the statistics panel after the analysis – recapitulated in “Parameters_analysis.txt”. These information include the number of trajectories after filtering, the number of trajectories found in the ROI, the number of trajectories used to quantify the diffusion coefficient and the density of the tracks in the ROI. If no ROI was selected, these numbers correspond to the whole field of view.

TROUBLESHOOTING

- 63) *MSD & Diffusion analysis: data-driven partitioning using Mixture Modeling (Steps 63-66)*. Organize the data as follow. The root directory is called “Test_Folder”. Within the root directory containing the data to be analyzed is named “Line_Condition”. One sub-directory represents one cell and initially contains a

single text file called “Saved_Diffusion_Coeff”, generated in step 59, with comma-separated columns and decimals encoded by a dot. Note that the R script (see Step 66) will create an additional sub-directory “pool” where all cells belonging to the same “Line_Condition” are pooled together in order to assess the presence of sub-populations and eventually set a threshold.

64) Open SPTpalm_Rscript in RStudio script editor (**Fig. 8a**).

65) Modify the parameters to be set by the user in the R script:

- line 14: absolute path of the root directory where are the datasets to be analyzed ("`~/Desktop/Test_Folder/`" for instance);
- line 15: dataset name, for instance type "EVECT2_Ctrl" (“Line_Condition”) for a single or `c("PIP2_Ctrl", "Lti6B_Ctrl", "EVECT2_Ctrl")` for multiple datasets, providing they are all located in the same Test_Folder root directory;
- line 17: number of bins for the histograms, set to 30 by default;
- line 18: type of mixture model, "GMM" classic gaussian mixture model or "FMSMSN" for skewed-gaussian mixture model (if both analyses are required, `c("GMM", "FMSMSN")`);
- threshold for the parameters CIs, set to 95% by default.

66) Run the script.

Critical step: The output files generated by the script will provide the following: two histograms of D_{inst} and $\log_{10}(D_{inst})$ per cell for each sub-directory are generated on the same panel in .tif (**Fig. 8b**). The created “pool” sub-directory contains the following files and plot. The “Saved_Diffusion_Coeff_pool” text file concatenates all D_{inst} and $\log_{10}(D_{inst})$ values per cell for the current dataset. The “summary” text file reports the parameter estimates from either the GMM or FMSMSN analysis as well as the BIC, the CIs, the MAP threshold and a Boolean indicated the best BIC-based model. For GMM, “X” refers to a single population, “E” and “V” stands for equal or variance-specific components. Note that all mixture models with 1 or 2 components are fit and reported whatever the best BIC-model is retained. A text file “classes_Diffusion_Coeff_pool” summarizes sub-populations obtained from the best BIC-based model - \leq MAP threshold, $>$ MAP threshold, all tracks - information for each cell and for the pool (group, number and proportion of tracks, mean and standard

deviation of $\log_{10}(D_{\text{inst}})$ in each subpopulation). Histograms of $\log_{10}(D_{\text{inst}})$ distributions pooled and per cell are displayed on the same .tif, overlaid with the color-coded density of the mixture components, the MAP threshold and the fraction of tracks classified in each component. A suffix, “_GMM” or “_FMSMSN”, is added to the two text files as well as the .tif to avoid that both types of analysis are overwritten.

Troubleshooting

Troubleshooting advice can be found in Table 3

Timing

Step 1-8, Coverslips cleaning: □45 minutes.

Step 9, Plant growing: 10 minutes to sow seed, 5 days growth

Step 10-13, Sample preparation: □45 minutes, more if multiple incubations are needed.

Step 14-34, Acquisition: 4 hours.

Step 35-55, Detection and reconnections: 4 hours (can be done overnight).

Step 56-66, MSD and Diffusion analysis: 5-8 hours.

Anticipated results: Analysis of molecules heterogeneity for a given genotype/condition

Overall, this protocol enables researchers to localize and to track individual molecules, and to describe their diffusion properties. As case studies, we here discuss 3 example proteins where latent sub-populations can be more or less easily distinguished by eye and we later emphasize the additional value of the MM framework.

First exploration with the viewer. Fig. 7 shows the sptPALM_viewer results obtained from one acquisition per genotype for roots expressing LTi6B-mEos2, PIP2;1-mEos2 or mEos2-PH^{EVECT2}. For Lti6B-mEos2, the distribution of $\log_{10}(D_{\text{inst}})$ seems to present a single major population of

relatively mobile molecules (average $\log_{10}(D_{\text{inst}})=-1.22$) (**Fig. 7a**), with the corresponding MSD curve and overlay of all tracks in **Fig. 7b** and **Fig. 7c**. For PIP2;1-mEos2, the distribution of $\log_{10}(D_{\text{inst}})$ also seems to present a single population though with a heavier right-tail than Lti6B-mEos2, but molecules are rather immobile ($\log_{10}(D_{\text{inst}})=-2.45$) (**Fig. 7d**). The MSD values over time are low, plateauing at roughly $5 \times 10^{-3} \mu\text{m}^2/\text{s}$ (**Fig. 7e**). For mEos2-PH^{EVECT2}, the variance of the $\log_{10}(D_{\text{inst}})$ distribution is clearly bigger than the other lines (**Fig. 7g**). In this example, the user should select the two sub-populations option in Step 59, which provides a starting threshold to separate both sub-populations and result in the fitting of a two-gaussian model. **Fig. 7h** displays the result of the fit (average $\log_{10}(D_{\text{inst}})=-1.23$, blue mobile partition, and average $\log_{10}(D_{\text{inst}})=-2.39$, orange immobile partition). The two corresponding MSD curves are given in **Fig. 7i**. **Fig. 7j** shows the overlay of all the tracks, which are color-coded for the two sub-populations in **Fig. 7k**. Note that the areas that correspond to the extracellular space have very few detected particles (stars).

Second step with the mixture model. We combined multiple acquisitions to perform formal statistical analysis using “SPTpalm_Rscript” with the data-driven MM framework (see Steps 63-66). Results are given in **Fig. 8** for mEos2-PH^{EVECT2} and **Extended Data Figure 3a and b** for Lti6B-mEos2 and **Extended Data Figure 3c and d** for PIP2;1-mEos2 (histograms from pooled cells only are shown, since the MM fit is done on pooled cells). **Fig. 8b** shows histograms of D_{inst} (left) and $\log_{10}(D_{\text{inst}})$ (right) for one cell and the MM model analysis is given in **Fig. 8c** (see figure legend). The best BIC-model is a GMM-2E, i.e. with 2 components of equal variance. In the example, the optimum $\log_{10}(D_{\text{inst}})$ threshold is -1.65 and partitions 45% of the molecules in a fast sub-populations of mean -1.15 with $\text{CI}_{95\%}=[-1.16, -1.13]$. For the 55% slow sub-population, the mean is -2.24 with $\text{CI}_{95\%}=[-2.25, -2.22]$. For Lti6B-mEos2 (**Extended Data Figure 3a**) and PIP2;1-mEos2 (**Extended Data Figure 3d**), GMM-2V and FMSMSN-2 reveal the presence of two sub-populations. For Lti6B-mEos2, the threshold of -1.63 splits 78% of the molecules in the fast sub-population with a mean of -1.25 ($\text{CI}_{95\%}=[-1.25, -1.24]$) and 22% in the slow sub-population with a mean of -1.48 ($\text{CI}_{95\%}=[-1.5, -1.47]$). The mean associated to the slowest component is higher than for mEos2-PH^{EVECT2}. For PIP2;1-mEos2, 90% of the molecules are assigned to the fast sub-population due to the presence of the heavy tail, with a similar threshold of -1.63, with means of -2.36 for the fast sub-population and -1.62 for the

(10%) slow sub-population. Note that it is up to the user to interpret the sub-populations. Though not retained, additional model outputs are given; FMSMSN-2 for Lti6b-mEos2 data and GMM-2E for PIP2;1-mEos2 in **Extended Data Figure 3b** and **d** respectively.

Acknowledgements:

We acknowledge the contribution of SFR Biosciences (UMS3444/CNRS, US8/Inserm, ENS de Lyon, UCBL) facilities: C. Lionnet, E. Chattré, and J. Brocard. Y.J. is funded by ERC no. 3363360-APPL under FP/2007-2013 and ANR caLIPSO (ANR18-CE13-0025); Y.J. and A.M. by the innovative project iRrobot from the department of “Biologie et Amélioration des Plantes” (BAP) of INRAE, A.M. is funded by the French National Agency ANR CellOsmo (ANR-19-CE20-0008-01), C.B. is funded by the Austrian Science Fund (FWF W1225). We acknowledge support by France-BioImaging (ANR-10-INBS-04, « Investments for the future »).

Competing interests statement

The authors have no competing interests as defined by Nature Research, or other interests that might be perceived to influence the interpretation of the article.

Author contributions:

V.B., M.P.P., and A.M. set-up the imaging conditions and performed imaging, J.B.F. established the sptPALM analysis pipeline and coded the sptPALM_viewer software, V.B., A.M. and J.B.F. performed image analyses, C.B. established the statistical analysis pipeline and performs statistics, V.B., J.B.F., C.B., M.P.P., M.N., A.M. and Y.J. wrote the manuscript.

Code availability statement:

The code used for the analysis of TrackMate or MTT data have been uploaded to <https://github.com/jbfiche/sptPALM/> and explanations on how to run an analysis can be found in the README.md file. A standalone application and a test-set are available from http://bioserv.cbs.cnrs.fr/DOWNLOAD/sptPALM_data/. Additional codes (including FIJI

plugins and R code for the statistics) as well as data used for the figures are accessible from http://bioserv.cbs.cnrs.fr/DOWNLOAD/sptPALM_data/. Additional advice on how to use them can be obtained from the authors upon reasonable request.

Data availability statement

All the raw data used to generate the Figures 4-8 and Extended Data Figures 1 to 3 are available at the following address: http://bioserv.cbs.cnrs.fr/DOWNLOAD/sptPALM_data/

Related links

Key references using this protocol:

1. Platre MP, et al. *Science*. 2019;364(6435):57-62. <https://doi.org/10.1126/science.aav9959>
2. Martinière A, et al. *Plant Physiol*. 2019;179(4):1581-1593. <https://doi.org/10.1104/pp.18.01065>
3. Smokvarska M, et al. *Curr Biol* 2020 Sep 29:S0960-9822(20)31344-0. doi: 10.1016/j.cub.2020.09.013

References:

- 1 Jacobson, K., Liu, P. & Lagerholm, B. C. The Lateral Organization and Mobility of Plasma Membrane Components. *Cell* **177**, 806-819, doi:10.1016/j.cell.2019.04.018 (2019).
- 2 Jaillais, Y. & Ott, T. The nanoscale organization of the plasma membrane and its importance in signaling - a proteolipid perspective. *Plant physiology*, pp.01349.02019, doi:10.1104/pp.19.01349 (2020).
- 3 Grossmann, G. *et al.* Green light for quantitative live-cell imaging in plants. *Journal of cell science* **131**, doi:10.1242/jcs.209270 (2018).
- 4 Donaldson, L. Autofluorescence in Plants. *Molecules* **25**, doi:10.3390/molecules25102393 (2020).
- 5 Wang, L., Xue, Y., Xing, J., Song, K. & Lin, J. Exploring the Spatiotemporal Organization of Membrane Proteins in Living Plant Cells. *Annual review of plant biology* **69**, 525-551, doi:10.1146/annurev-arplant-042817-040233 (2018).
- 6 Cui, Y. *et al.* Single-Particle Tracking for the Quantification of Membrane Protein Dynamics in Living Plant Cells. *Molecular plant* **11**, 1315-1327, doi:10.1016/j.molp.2018.09.008 (2018).
- 7 Wang, L. *et al.* Spatiotemporal Dynamics of the BRI1 Receptor and its Regulation by Membrane Microdomains in Living Arabidopsis Cells. *Molecular plant* **8**, 1334-1349, doi:10.1016/j.molp.2015.04.005 (2015).
- 8 Wang, X. *et al.* Single-molecule fluorescence imaging to quantify membrane protein dynamics and oligomerization in living plant cells. *Nature protocols* **10**, 2054-2063, doi:10.1038/nprot.2015.132 (2015).

- 9 Hao, H. *et al.* Clathrin and Membrane Microdomains Cooperatively Regulate RbohD Dynamics and Activity in Arabidopsis. *The Plant cell* **26**, 1729-1745, doi:10.1105/tpc.113.122358 (2014).
- 10 Li, X. *et al.* Single-molecule analysis of PIP2;1 dynamics and partitioning reveals multiple modes of Arabidopsis plasma membrane aquaporin regulation. *The Plant cell* **23**, 3780-3797, doi:10.1105/tpc.111.091454 (2011).
- 11 Wang, Q. *et al.* Single-particle analysis reveals shutoff control of the Arabidopsis ammonium transporter AMT1;3 by clustering and internalization. *Proceedings of the National Academy of Sciences of the United States of America* **110**, 13204-13209, doi:10.1073/pnas.1301160110 (2013).
- 12 McKenna, J. F. *et al.* The cell wall regulates dynamics and size of plasma-membrane nanodomains in Arabidopsis. *Proceedings of the National Academy of Sciences of the United States of America* **116**, 12857-12862, doi:10.1073/pnas.1819077116 (2019).
- 13 Martiniere, A. *et al.* Cell wall constrains lateral diffusion of plant plasma-membrane proteins. *Proceedings of the National Academy of Sciences of the United States of America* **109**, 12805-12810, doi:10.1073/pnas.1202040109 (2012).
- 14 Platre, M. P. *et al.* Developmental control of plant Rho GTPase nano-organization by the lipid phosphatidylserine. *Science* **364**, 57-62, doi:10.1126/science.aav9959 (2019).
- 15 Martiniere, A. *et al.* Osmotic Stress Activates Two Reactive Oxygen Species Pathways with Distinct Effects on Protein Nanodomains and Diffusion. *Plant physiology* **179**, 1581-1593, doi:10.1104/pp.18.01065 (2019).
- 16 Hosy, E., Martiniere, A., Choquet, D., Maurel, C. & Luu, D. T. Super-resolved and dynamic imaging of membrane proteins in plant cells reveal contrasting kinetic profiles and multiple confinement mechanisms. *Molecular plant* **8**, 339-342, doi:10.1016/j.molp.2014.10.006 (2015).
- 17 Simon, M. L. *et al.* A PtdIns(4)P-driven electrostatic field controls cell membrane identity and signalling in plants. *Nat Plants* **2**, 16089, doi:10.1038/nplants.2016.89 (2016).
- 18 Li, X., Xing, J., Qiu, Z., He, Q. & Lin, J. Quantification of Membrane Protein Dynamics and Interactions in Plant Cells by Fluorescence Correlation Spectroscopy. *Molecular plant* **9**, 1229-1239, doi:10.1016/j.molp.2016.06.017 (2016).
- 19 Gronnier, J. *et al.* Structural basis for plant plasma membrane protein dynamics and organization into functional nanodomains. *eLife* **6**, doi:10.7554/eLife.26404 (2017).
- 20 Perraki, A. *et al.* REM1.3's phospho-status defines its plasma membrane nanodomain organization and activity in restricting PVX cell-to-cell movement. *PLoS pathogens* **14**, e1007378, doi:10.1371/journal.ppat.1007378 (2018).
- 21 Smokvarska, M. *et al.* A Plasma Membrane Nanodomain Ensures Signal Specificity during Osmotic Signaling in Plants. *Current biology : CB*, doi:10.1016/j.cub.2020.09.013 (2020).
- 22 Manley, S. *et al.* High-density mapping of single-molecule trajectories with photoactivated localization microscopy. *Nature methods* **5**, 155-157, doi:10.1038/nmeth.1176 (2008).
- 23 Baddeley, D. & Bewersdorf, J. Biological Insight from Super-Resolution Microscopy: What We Can Learn from Localization-Based Images. *Annu Rev Biochem* **87**, 965-989, doi:10.1146/annurev-biochem-060815-014801 (2018).
- 24 Betzig, E. *et al.* Imaging intracellular fluorescent proteins at nanometer resolution. *Science* **313**, 1642-1645, doi:10.1126/science.1127344 (2006).
- 25 Thompson, R. E., Larson, D. R. & Webb, W. W. Precise nanometer localization analysis for individual fluorescent probes. *Biophysical journal* **82**, 2775-2783, doi:10.1016/s0006-3495(02)75618-x (2002).
- 26 Schermelleh, L. *et al.* Super-resolution microscopy demystified. *Nature cell biology* **21**, 72-84, doi:10.1038/s41556-018-0251-8 (2019).

- 27 Li, Y. *et al.* Real-time 3D single-molecule localization using experimental point spread functions. *Nature methods* **15**, 367-369, doi:10.1038/nmeth.4661 (2018).
- 28 Huang, B., Wang, W., Bates, M. & Zhuang, X. Three-dimensional super-resolution imaging by stochastic optical reconstruction microscopy. *Science* **319**, 810-813, doi:10.1126/science.1153529 (2008).
- 29 Siemons, M. *et al.* Comparing strategies for deep astigmatism-based single-molecule localization microscopy. *Biomed. Opt. Express* **11**, 735-751, doi:10.1364/BOE.382023 (2020).
- 30 Izeddin, I. *et al.* PSF shaping using adaptive optics for three-dimensional single-molecule super-resolution imaging and tracking. *Opt. Express* **20**, 4957-4967, doi:10.1364/OE.20.004957 (2012).
- 31 Shechtman, Y., Sahl, S. J., Backer, A. S. & Moerner, W. E. Optimal point spread function design for 3D imaging. *Physical review letters* **113**, 133902, doi:10.1103/PhysRevLett.113.133902 (2014).
- 32 Zhang, X. *et al.* Phosphorylation-Mediated Dynamics of Nitrate Transceptor NRT1.1 Regulate Auxin Flux and Nitrate Signaling in Lateral Root Growth. *Plant physiology* **181**, 480-498, doi:10.1104/pp.19.00346 (2019).
- 33 Xing, J. *et al.* Secretion of Phospholipase D δ Functions as a Regulatory Mechanism in Plant Innate Immunity. *The Plant cell* **31**, 3015-3032, doi:10.1105/tpc.19.00534 (2019).
- 34 Zhao, Y., Man, Y., Wen, J., Guo, Y. & Lin, J. Advances in Imaging Plant Cell Walls. *Trends in plant science* **24**, 867-878, doi:10.1016/j.tplants.2019.05.009 (2019).
- 35 Zhang, X., Cui, Y., Yu, M. & Lin, J. Single-Molecule Techniques for Imaging Exo-Endocytosis Coupling in Cells. *Trends in plant science* **24**, 879-880, doi:10.1016/j.tplants.2019.05.013 (2019).
- 36 Yu, M. *et al.* The dynamics and endocytosis of Flot1 protein in response to flg22 in Arabidopsis. *Journal of plant physiology* **215**, 73-84, doi:10.1016/j.jplph.2017.05.010 (2017).
- 37 Wudick, M. M. *et al.* Subcellular Redistribution of Root Aquaporins Induced by Hydrogen Peroxide. *Molecular plant* **8**, 1103-1114, doi:10.1016/j.molp.2015.02.017 (2015).
- 38 Cui, Y. *et al.* Sterols regulate endocytic pathways during flg22-induced defense responses in Arabidopsis. *Development* **145**, doi:10.1242/dev.165688 (2018).
- 39 Gronnier, J. *et al.* FERONIA regulates FLS2 plasma membrane nanoscale dynamics to modulate plant immune signaling. *bioRxiv*, 2020.2007.2020.212233, doi:10.1101/2020.07.20.212233 (2020).
- 40 Johnson, A. & Vert, G. Single Event Resolution of Plant Plasma Membrane Protein Endocytosis by TIRF Microscopy. *Frontiers in plant science* **8**, 612, doi:10.3389/fpls.2017.00612 (2017).
- 41 Johnson, A. *et al.* Experimental toolbox for quantitative evaluation of clathrin-mediated endocytosis in the plant model Arabidopsis. *Journal of cell science* **133**, doi:10.1242/jcs.248062 (2020).
- 42 Konopka, C. A., Backues, S. K. & Bednarek, S. Y. Dynamics of Arabidopsis dynamin-related protein 1C and a clathrin light chain at the plasma membrane. *The Plant cell* **20**, 1363-1380, doi:10.1105/tpc.108.059428 (2008).
- 43 Konopka, C. A. & Bednarek, S. Y. Variable-angle epifluorescence microscopy: a new way to look at protein dynamics in the plant cell cortex. *The Plant journal : for cell and molecular biology* **53**, 186-196, doi:10.1111/j.1365-313X.2007.03306.x (2008).
- 44 Wan, Y., Xue, Y., Li, R. & Lin, J. Application of Variable Angle Total Internal Reflection Fluorescence Microscopy to Investigate Protein Dynamics in Intact Plant Cells. *Methods Mol Biol* **1363**, 123-132, doi:10.1007/978-1-4939-3115-6_10 (2016).

- 45 Serge, A., Bertaux, N., Rigneault, H. & Marguet, D. Dynamic multiple-target tracing to probe spatiotemporal cartography of cell membranes. *Nature methods* **5**, 687-694, doi:10.1038/nmeth.1233 (2008).
- 46 Rouger, V. *et al.* Mapping molecular diffusion in the plasma membrane by Multiple-Target Tracing (MTT). *J Vis Exp*, e3599, doi:10.3791/3599 (2012).
- 47 Durand-Smet, P., Spelman, T. A., Meyerowitz, E. M. & Jönsson, H. Cytoskeletal organization in isolated plant cells under geometry control. *Proceedings of the National Academy of Sciences of the United States of America* **117**, 17399-17408, doi:10.1073/pnas.2003184117 (2020).
- 48 Los, G. V. *et al.* HaloTag: a novel protein labeling technology for cell imaging and protein analysis. *ACS chemical biology* **3**, 373-382, doi:10.1021/cb800025k (2008).
- 49 Chen, J. *et al.* Single-molecule dynamics of enhanceosome assembly in embryonic stem cells. *Cell* **156**, 1274-1285, doi:10.1016/j.cell.2014.01.062 (2014).
- 50 Holcman, D. *et al.* Single particle trajectories reveal active endoplasmic reticulum luminal flow. *Nature cell biology* **20**, 1118-1125, doi:10.1038/s41556-018-0192-2 (2018).
- 51 Jin, D. *et al.* Nanoparticles for super-resolution microscopy and single-molecule tracking. *Nature methods* **15**, 415-423, doi:10.1038/s41592-018-0012-4 (2018).
- 52 Banaz, N., Mäkelä, J. & Uphoff, S. Choosing the right label for single-molecule tracking in live bacteria: side-by-side comparison of photoactivatable fluorescent protein and Halo tag dyes. *J Phys D Appl Phys* **52**, 064002, doi:10.1088/1361-6463/aaf255 (2019).
- 53 Varela, J. A. *et al.* Single nanoparticle tracking of [Formula: see text]-methyl-d-aspartate receptors in cultured and intact brain tissue. *Neurophotonics* **3**, 041808, doi:10.1117/1.NPh.3.4.041808 (2016).
- 54 Varela, J. A. *et al.* Targeting neurotransmitter receptors with nanoparticles in vivo allows single-molecule tracking in acute brain slices. *Nature communications* **7**, 10947, doi:10.1038/ncomms10947 (2016).
- 55 Freeman, S. A. *et al.* Transmembrane Pickets Connect Cyto- and Pericellular Skeletons Forming Barriers to Receptor Engagement. *Cell* **172**, 305-317 e310, doi:10.1016/j.cell.2017.12.023 (2018).
- 56 Groc, L. *et al.* Surface trafficking of neurotransmitter receptor: comparison between single-molecule/quantum dot strategies. *The Journal of neuroscience : the official journal of the Society for Neuroscience* **27**, 12433-12437, doi:10.1523/jneurosci.3349-07.2007 (2007).
- 57 Liu, H. *et al.* Visualizing long-term single-molecule dynamics in vivo by stochastic protein labeling. *Proceedings of the National Academy of Sciences of the United States of America* **115**, 343-348, doi:10.1073/pnas.1713895115 (2018).
- 58 Grimm, J. B. *et al.* Bright photoactivatable fluorophores for single-molecule imaging. *Nature methods* **13**, 985-988, doi:10.1038/nmeth.4034 (2016).
- 59 Iwatate, R. J. *et al.* Covalent Self-Labeling of Tagged Proteins with Chemical Fluorescent Dyes in BY-2 Cells and Arabidopsis Seedlings. *The Plant cell* **32**, 3081-3094, doi:10.1105/tpc.20.00439 (2020).
- 60 Lippincott-Schwartz, J., Altan-Bonnet, N. & Patterson, G. H. Photobleaching and photoactivation: following protein dynamics in living cells. *Nature cell biology* **Suppl**, S7-14 (2003).
- 61 Kang, M., Day, C. A., Kenworthy, A. K. & DiBenedetto, E. Simplified equation to extract diffusion coefficients from confocal FRAP data. *Traffic* **13**, 1589-1600, doi:10.1111/tra.12008 (2012).
- 62 Wawrezynieck, L., Rigneault, H., Marguet, D. & Lenne, P. F. Fluorescence correlation spectroscopy diffusion laws to probe the submicron cell membrane organization. *Biophysical journal* **89**, 4029-4042, doi:10.1529/biophysj.105.067959 (2005).

- 63 Xiang, L., Chen, K., Yan, R., Li, W. & Xu, K. Single-molecule displacement mapping unveils nanoscale heterogeneities in intracellular diffusivity. *Nature methods*, doi:10.1038/s41592-020-0793-0 (2020).
- 64 Lenne, P. F. *et al.* Dynamic molecular confinement in the plasma membrane by microdomains and the cytoskeleton meshwork. *The EMBO journal* **25**, 3245-3256, doi:10.1038/sj.emboj.7601214 (2006).
- 65 Rose, M., Hirmiz, N., Moran-Mirabal, J. M. & Fradin, C. Lipid Diffusion in Supported Lipid Bilayers: A Comparison between Line-Scanning Fluorescence Correlation Spectroscopy and Single-Particle Tracking. *Membranes* **5**, 702-721, doi:10.3390/membranes5040702 (2015).
- 66 Hosy, E., Martiniere, A., Choquet, D., Maurel, C. & Luu, D. T. Super-resolved and dynamic imaging of membrane proteins in plant cells reveal contrasting kinetic profiles and multiple confinement mechanisms. *Molecular plant*, doi:10.1093/mp/ssu123 (2014).
- 67 Sibarita, J. B. High-density single-particle tracking: quantifying molecule organization and dynamics at the nanoscale. *Histochem Cell Biol* **141**, 587-595, doi:10.1007/s00418-014-1214-1 (2014).
- 68 McKinney, S. A., Murphy, C. S., Hazelwood, K. L., Davidson, M. W. & Looger, L. L. A bright and photostable photoconvertible fluorescent protein. *Nature methods* **6**, 131-133, doi:10.1038/nmeth.1296 (2009).
- 69 Zhang, M. *et al.* Rational design of true monomeric and bright photoactivatable fluorescent proteins. *Nature methods* **9**, 727-729, doi:10.1038/nmeth.2021 (2012).
- 70 De Zitter, E. *et al.* Mechanistic investigation of mEos4b reveals a strategy to reduce track interruptions in sptPALM. *Nature methods* **16**, 707-710, doi:10.1038/s41592-019-0462-3 (2019).
- 71 Subach, F. V., Patterson, G. H., Renz, M., Lippincott-Schwartz, J. & Verkhusa, V. V. Bright monomeric photoactivatable red fluorescent protein for two-color super-resolution sptPALM of live cells. *Journal of the American Chemical Society* **132**, 6481-6491, doi:10.1021/ja100906g (2010).
- 72 Durisic, N., Laparra-Cuervo, L., Sandoval-Alvarez, A., Borbely, J. S. & Lakadamyali, M. Single-molecule evaluation of fluorescent protein photoactivation efficiency using an in vivo nanotemplate. *Nature methods* **11**, 156-162, doi:10.1038/nmeth.2784 (2014).
- 73 Dahlberg, P. D. *et al.* Identification of PAmKate as a Red Photoactivatable Fluorescent Protein for Cryogenic Super-Resolution Imaging. *Journal of the American Chemical Society* **140**, 12310-12313, doi:10.1021/jacs.8b05960 (2018).
- 74 Hussein, W. & Berlin, S. Red Photoactivatable Genetic Optical-Indicators. *Frontiers in Cellular Neuroscience* **14**, doi:10.3389/fncel.2020.00113 (2020).
- 75 van de Linde, S. Single-molecule localization microscopy analysis with ImageJ. *Journal of Physics D: Applied Physics* **52**, 203002, doi:10.1088/1361-6463/ab092f (2019).
- 76 Tinevez, J. Y. *et al.* TrackMate: An open and extensible platform for single-particle tracking. *Methods* **115**, 80-90, doi:10.1016/j.ymeth.2016.09.016 (2017).
- 77 Schindelin, J. *et al.* Fiji: an open-source platform for biological-image analysis. *Nature methods* **9**, 676-682, doi:10.1038/nmeth.2019 (2012).
- 78 Schneider, C. A., Rasband, W. S. & Eliceiri, K. W. NIH Image to ImageJ: 25 years of image analysis. *Nature methods* **9**, 671-675, doi:10.1038/nmeth.2089 (2012).
- 79 Kao, H. P. & Verkman, A. S. Tracking of single fluorescent particles in three dimensions: use of cylindrical optics to encode particle position. *Biophysical journal* **67**, 1291-1300, doi:10.1016/S0006-3495(94)80601-0 (1994).
- 80 Gebhardt, J. C. M. *et al.* Single-molecule imaging of transcription factor binding to DNA in live mammalian cells. *Nature methods* **10**, 421-426, doi:10.1038/nmeth.2411 (2013).
- 81 Izeddin, I. *et al.* Single-molecule tracking in live cells reveals distinct target-search strategies of transcription factors in the nucleus. *eLife* **3**, doi:10.7554/eLife.02230 (2014).

- 82 Kusumi, A., Sako, Y. & Yamamoto, M. Confined lateral diffusion of membrane receptors as studied by single particle tracking (nanovid microscopy). Effects of calcium-induced differentiation in cultured epithelial cells. *Biophysical journal* **65**, 2021-2040, doi:10.1016/s0006-3495(93)81253-0 (1993).
- 83 Wieser, S. & Schutz, G. J. Tracking single molecules in the live cell plasma membrane-Do's and Don't's. *Methods* **46**, 131-140, doi:10.1016/j.ymeth.2008.06.010 (2008).
- 84 Michalet, X. Mean square displacement analysis of single-particle trajectories with localization error: Brownian motion in an isotropic medium. *Phys Rev E Stat Nonlin Soft Matter Phys* **82**, 041914, doi:10.1103/PhysRevE.82.041914 (2010).
- 85 Deschout, H. *et al.* Precisely and accurately localizing single emitters in fluorescence microscopy. *Nature methods* **11**, 253-266, doi:10.1038/nmeth.2843 (2014).
- 86 Reynolds, D. A. Gaussian Mixture Models. *Encyclopedia of biometrics* **741** (2009).
- 87 Dempster, A. P., Laird, N. M. & Rubin, D. B. Maximum likelihood from incomplete data via the EM algorithm. *Journal of the Royal Statistical Society: Series B (Methodological)* **39**, 1-22 (1977).
- 88 Azzalini, A. A Class of Distributions Which Includes the Normal Ones. *Scandinavian Journal of Statistics* **12**, 171-178 (1985).
- 89 Prates, M. O., Lachos, V. H. & Barbosa Cabral, C. R. mixsmsn: Fitting Finite Mixture of Scale Mixture of Skew-Normal Distributions. *2013* **54**, 20, doi:10.18637/jss.v054.i12 (2013).
- 90 Dowle, M. *et al.* Package 'data.table'. *Extension of 'data.frame'* (2019).
- 91 Scrucca, L., Fop, M., Murphy, T. B. & Raftery, A. E. mclust 5: Clustering, Classification and Density Estimation Using Gaussian Finite Mixture Models. *The R journal* **8**, 289-317 (2016).
- 92 Mattheyses, A. L., Shaw, K. & Axelrod, D. Effective elimination of laser interference fringing in fluorescence microscopy by spinning azimuthal incidence angle. *Microscopy Research and Technique* **69**, 642-647, doi:10.1002/jemt.20334 (2006).
- 93 Fiolka, R., Belyaev, Y., Ewers, H. & Stemmer, A. Even illumination in total internal reflection fluorescence microscopy using laser light. *Microscopy Research and Technique* **71**, 45-50, doi:10.1002/jemt.20527 (2008).
- 94 Levet, F. *et al.* SR-Tesseler: a method to segment and quantify localization-based super-resolution microscopy data. *Nature methods* **12**, 1065-1071, doi:10.1038/nmeth.3579 (2015).
- 95 Milo, R. & Phillips, R. What are the time scales for diffusion in cells? in *Cell Biology by the Numbers*. (ed Garland Science) 256-260 (2016).

Figure legends:

Figure 1: Schematic representation of sptPALM. (a-b) During image acquisition, images are taken every 20 ms for the duration of 3 min. Top view (a) and side view (b). In each image, only a few, well separated emitters (red dots) are detected. (c) Using tracking and localization methods, it is then possible to obtain the super-resolved trajectories of single molecules. Figure modified from¹⁴.

Figure 2: Comparison of the typical dynamic range of FRAP, FCS, sptPALM and SMdM. The section at the top shows the dynamic range of FRAP, FCS, sptPALM and SMdM for studying protein diffusion in cells. The section at the bottom, shows the typical dynamic range of membrane proteins and free cytosolic proteins⁹⁵. Note that the dynamic range to estimate diffusion by sptPALM fits well with the typical diffusion of most plasma membrane proteins but not free cytosolic proteins.

Figure 3: Coverslip cleaning and sample preparation. (a) Picture and schematic of coverslips organization in the rack and (b) the staining jar. For the cleaning procedure, see Step 1-8. (c) Schematic view of the 12-well plate filled with C control medium, M Mock and T treatment medium (Step 10-11). (d) Picture showing a droplet of medium on a dirty (left) and a cleaned (right) coverslip (Step 12). The filter paper is maintained on the bench using surgical tape (Step 12). (e) Schematic and (f) picture showing how to position roots samples placed in the middle of the coverslip (Step 13), perpendicularly to its main axis, and with the microscope slide on the top. Tape on both sides of the coverslip ensure proper assembly and spacing.

Figure 4: sptPALM track acquisition. (a) Typical image obtained with low (below 0.001% laser intensity) or no 405-nm laser photo-conversion. Note that few spots are visible. (b) Image with a good photo-conversion (usually between 0.01 and 0.1% of 405-nm laser power —0.1 to 1.03 μ W at the objective) resulting in an acceptable number of molecules per frame, here 17 (Step 22). In (c), 405-nm laser power was increased to 0.02%. The number of particles is still in a good range (21) but some are too close to each other, creating false reconnections during track reconstruction. (d) Enlarged view of the area marked c. (e) Image corresponding to a Z-Stack Max intensity projection of 1,000 frames obtained using ImageJ. This view is useful to visualize the cell outline. No signal should be detected outside of the cell (Step 30). (f) Image corresponding to a Z-Stack Mean intensity projection obtained using ImageJ and allowing to evaluate the cellular background and unspecific dotty signals (Step 31). (g) close-up view of a spot. A straight line has been drawn across it and the ImageJ surface plot tool (h) was used to evaluate the maximum pixel value of a particle (here 11,600 units) (Step 23). Note that cells in (a), (b) and (c) are from different acquisitions whereas (e) and (f) are projections of the time-lapse from (b). Scale bars in (a-c), (e) and (f) 5 μ m; scale bar in (d) 2 μ m and scale bar in (g) 1 μ m. All the source data are available from: http://bioserv.cbs.cnrs.fr/DOWNLOAD/sptPALM_data/

Figure 5: Track reconstruction using MTT. (a) Screenshot of MTT mode and date selection (Step 38). (b) Screenshot of the MTT software interface (Step 41). (c) Time-lapse loaded to determine the Alpha threshold (Step 43). (d) Detected tracks overlaid to

the time-lapse (Step 44). Here for an Alpha threshold set up at 1,000. All the source data are available from: http://bioserv.cbs.cnrs.fr/DOWNLOAD/sptPALM_data/

Figure 6: MSD & Diffusion analysis using the sptPALM_viewer software. (a) Screenshot of the sptPALM_viewer software interface (Step 45). (b) Cumulative distribution of step length obtained after loading MTT/TrackMate files with different upper thresholds (no threshold and 99.5th, 99th, 98.5th, 98th percentiles, see legend). (c) Normalized histogram of trajectories duration (s) with either 80th (green dotted line) or 90th (red dotted line) percentiles. (d) Visualization of tracks. The color gradient from blue, green to red indicates the early to late recorded positions (Step 49). All the source data are available from: http://bioserv.cbs.cnrs.fr/DOWNLOAD/sptPALM_data/

Figure 7: MSD & Diffusion results from the sptPALM_viewer. Data shown are obtained for one acquisition, which includes between one to three cells. (a) Normalized histogram (bin=0.05) of $\log_{10}(D_{inst})$ for Lti6B-mEos2 (n=4,409/10,216), (b) corresponding average of median (+/-SE) MSD over time, and (c) overlay of the trajectories (Step 59). (d-e) same as (a-c) for PIP2;1-mEos2 (n=4,841/9,714) (Step 59). (g-h) Normalized histogram (bin=0.05) of $\log_{10}(D_{inst})$ for mEos2-PH^{EVECT2} (n=2,368/7,869) without (g) and after a two-gaussian fitting (h) (Step 60). In (h), the scaled densities of the two corresponding Gaussians are added and a color code identifies the two sub-populations; blue (orange) for relatively immobile (mobile) tracks. (i) Average of median (+/-SE) MSD over time after the partitioning of the mEos2-PH^{EVECT2} tracks into two populations, blue (orange) for relatively immobile (mobile) tracks. (j) overlay of the mEos2-PH^{EVECT2} trajectories and (k) overlay of the mEos2-PH^{EVECT2} trajectories after the partitioning of the mEos2-PH^{EVECT2} tracks into two populations, blue (orange) for relatively immobile (mobile) tracks (Step 61). Stars in (c), (f) and (j) show extracellular spaces between cells. Scale bars in (c), (f) and (j) are 1 μ m). In (a), (d) and (g), n is the number of molecules kept after filtering for the blinking and duration parameters, over the total number of tracks reconstructed by MTT. All the source data are available from: http://bioserv.cbs.cnrs.fr/DOWNLOAD/sptPALM_data/

Figure 8: Mixture modeling reveals two latent sub-populations of mEos2-PH^{EVECT2} molecules. (a) RStudio interface splitted in “Script”, “Console” and “Environment/File/Plot/Packages/Help” sections (Step 64). (b) Histograms for D_{inst} and $\log_{10}(D_{inst})$ plots obtained for 1 cell expressing mEos2-PH^{EVECT2}, and displayed for each cell in (c) (30 equally spaced bins by default). (c) MM analysis from pooled 6 cells (“hist_log10D_pool_suffix” .tif output with “suffix” type of the model). Top right: histogram of $\log_{10}(D_{inst})$ from pooled cells, with the components density of the best BIC MM plotted (GMM-2E here). Vertical black line indicates the optimal $\log_{10}(D_{inst})$ threshold and partitions mobile (orange) and immobile (blue) molecules. The dots indicate the estimated means of the MM. n corresponds to the number of molecules kept after filtering for the blinking and duration parameters. All the source data are available from: http://bioserv.cbs.cnrs.fr/DOWNLOAD/sptPALM_data/

Extended Data Figure 1. Fluorescence intensity of a typical mEOS2 sub-diffractive spot along time. (a) pictures showing a single molecule through time (20 ms between each picture) and (b) corresponding trace of fluorescent intensity. Note that the signal intensity observed is not continuous and the OFF state varies in duration between seconds and milliseconds. This blinking behavior is typical of single-molecule observation. Scale bar 1 μm .

Extended Data Figure 2 Example of false tracks identification. (a) Example of mis-reconnected tracks (white arrow). (b) Example of track with a very long duration (white arrowhead), indicating that it is background fluorescence rather than true signal. The color gradient from blue, green to red indicates the early vs late recorded positions. Scale bars are 1 μm .

Extended Data Figure 3. Mixture modeling reveals two latent sub-populations of Lti6B-mEos2 and PIP2;1-mEos2 molecules. GMM (a and c) and FMSMSN fits (b and d). Either a GMM-2V (a) or FMSMSN-2 (d) model is retained for Lti6b and PIP2;1 respectively, using the BIC criterion. See legend Fig.8c for more details.

Tables

Table 1: MTT parameters for track reconstructions

Parameters	Definition	How to set up
Threshold for the first detection	Threshold for the detection statistical test (likelihood of having a true particle or noise)	This parameter is usually set between 20 and 30. It is evaluated and optimized based on the particles detected from a calibration movie
Threshold for the last detection	Threshold for the detection statistical test (likelihood of having a true particle or noise)	Last detection for un-reconnected orphan peaks. Since the trajectories are usually small for sptPALM, this parameter is usually the same than for the first detection.
Size of the window	Size of the window for particle detection and background noise estimation	The default value of this parameter (7x7 pixels) is optimal for single molecule detection

Gaussian Radius	Standard deviation of the Gaussian characterizing the intensity distribution of the detected particle	For a single molecule, the standard deviation is equal to $\sim 190\text{nm}$. This parameter needs to be calculated according to the pixel size of the setup.
Weight of the alpha likelihood	-	The default value of this parameter is optimal for single molecule detection
Likelihood weight between the maximum and the local diffusion	-	The default value of this parameter is optimal for single molecule detection
Size of the temporal sliding window	Length of the temporal window (in frames) to compute local diffusion coefficient	The default value (5 frames) works well for sptPALM data
Number of deflation loop	Number of times the detection process will be repeated in order to detect low intensity events	Deflation loop is set to 0 in the case of sptPALM experiment.
Probability of blinking	Number of consecutive frame without detection for a given track	We usually set this parameters between 0 (no missing detection) to -3 (3 consecutive missing detection). The smaller is the blinking, the longer are the reconstructed tracks.
Coefficient of free diffusion	Maximum diffusion coefficient expected for the sample	We set the maximum coefficient of free diffusion at $1\mu\text{m}^2/\text{s}$, which corresponds to the upper limit of diffusion observed for PM protein in plant. This parameter could be adjusted depending of the sample and set according to results obtained on control experiments
Diameter to research the set particle	Maximum cutoff distance separating two consecutive events	This parameter has to be set according to the previous one and the acquisition time used for the acquisition. We

		classically set this parameter between 2.5-3.5 pixels, which corresponds to a maximal diffusion of ~0.5-0.8- $\mu\text{m}^2/\text{s}$ for an acquisition time of 20ms)
Number restricting the combinations	-	The default value of this parameter is optimal for single molecule detection
Alpha threshold	Initial threshold for particle detection (based on local intensity and noise)	This parameter is usually set between 50 and 500. It has to be optimized based on the detection obtain on image

Table 2: PALM_viewer parameters for track filtering and MSD analysis.

Parameters:	Definitions:	How to set up:
Acquisition time	Exposure time during acquisition in ms	Usually set at 20 ms. Exposure time must be high enough to obtain good S/B ratio. However too high exposure time might lead to deformed blurry PSF and trouble in track reconstructions
Pixel size	Size of the pixel in μm	This parameter can be retrieved in the acquisition software or in image metadata.
Maximum distance between two detections	Longest distance allowed between two consecutive detections (in μm)	Have to be adjusted depending of the reconnection errors and based on the cumulative distribution of single-step length. By default, this parameter is void.
Maximum of blinks (frames)	Number of consecutive frames without detections	High number of blinks increase the track length, but also possible reconnection errors. We used 3 as a default value.
Minimum trajectory duration (frames)	Minimum tracks duration (in frame)	Minimal track length has to be long enough to permit a good estimation of the MSD. The default value is 7 frames.

Analysis method	Indicate the method used to estimate the diffusion coefficient D	Two methods are available (Average and Fit). Both are based on an estimation of the MSD curve for each track. The average method is computationally less demanding than the fit. However, it is also less precise for diffusion coefficient $<0.01\mu\text{m}^2/\text{s}$.
Number of points used for D estimation	Number of points from the MSD curve that are used to estimate the diffusion coefficient D	Whatever the analysis method, this parameter is indicating the number of points from the MSD curve that are used to infer the diffusion coefficient. By default, this parameter is set to 4.
Maximum display time for MSD (s)	Maximum range of time on which the MSD curve will be plotted.	The trajectories measured by sptPALM being quite small, the default value is set to 0.5s for an acquisition time of 20ms.

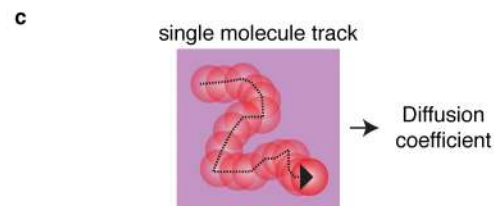
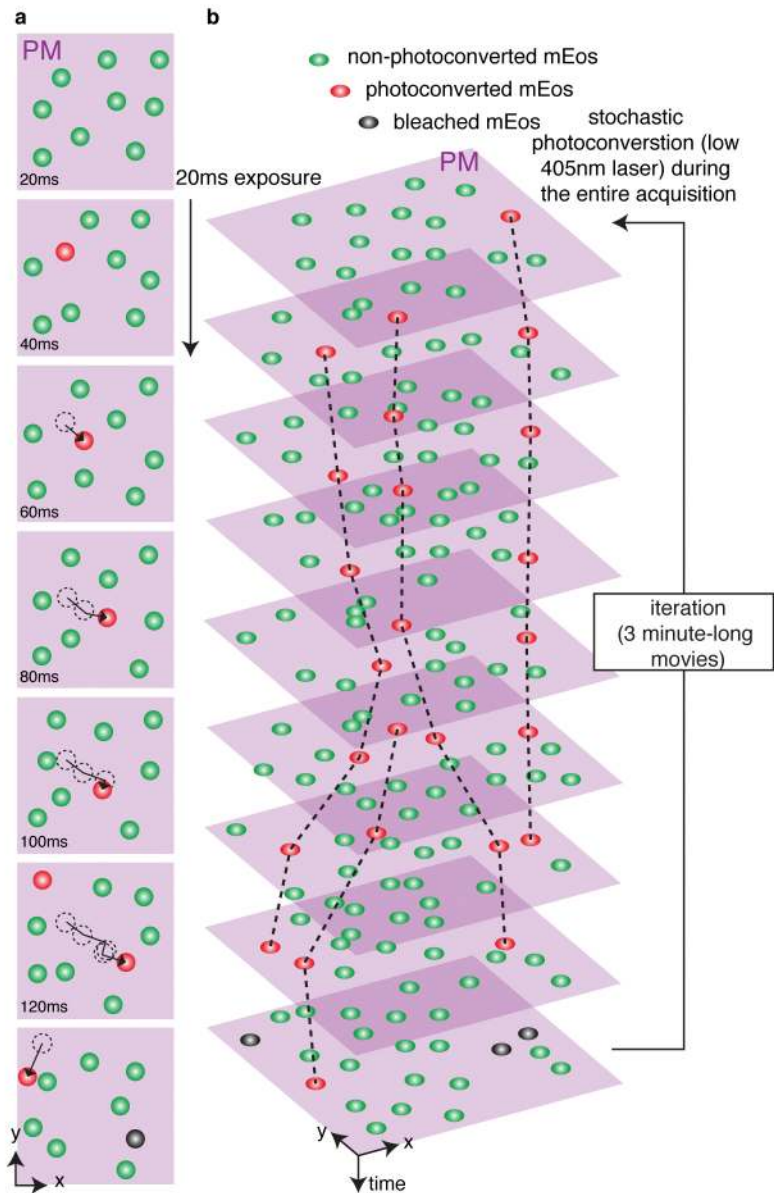
Table 3: Troubleshooting Table

Step	Problem	Possible causes	Solution
8	Coverslips breaks	Bunsen burner flame heat is too high or time within the flame is too long	Turn the Bunsen burner collar down or reduce the time within the flame to let the coverslip to cool down before passing through again
	Coverslips shows residues	Bunsen burner flame heat is too low	Turn the Bunsen burner collar up to get a blue flame

14-34	Homogenous background on the coverslip	Dirty coverslips/slides	If background persist using ultrapure water instead use filtered buffer, repeat Step 1-8 and use a new stock of slides
		Medium contamination	Prepare new filtered medium
		Crushed sample	Check sample integrity under transmitted light. Be gentle during sample manipulation/incubation/ transfer to the coverslip. Add a spacer in between slide and coverslips.
Low Signal /Background ratio	TIRF angle is not properly adjusted	Setup TIRF angle: Set the angle in epifluorescence (<math><60^\circ</math> in our setup) and then increase it to reach TIRF range (63-73°) with the highest S/B ratio possible.	
	Poor activation of photoconverted fluorophores	Increase Camera gain. Increasing 561nm laser power might help but it will also increase in unspecific background and moreover it will photobleach the fluorophores. Ultimately, acquisition time can be increased.	
Drift during acquisition	Sample movement in XY or Z axis during time-lapse	Discard acquisition. Fiducial marker can be added on the coverslip (Step 13) to correct drift in a post-acquisition treatment	
Low molecule density during acquisition	Low expression level	If tagged protein is expressed under the control of its own endogenous promoter, it might be necessary to switch for a more ubiquitous promoter such as Ubiquitin10 or 35S promoters	

		Low photoconversion	Increase UV laser power
	High molecules density during acquisition	High photoconversion/excitation	Decrease UV or 561nm laser power.
56-62	False track identification (Extended Data Figure 2)	Reconnection errors. Straight lines connecting two points above a certain distance	They can be removed by reducing the maximum distance between two detections threshold. Usually, taking an extreme quantile of the distribution of distance between two detections over all tracks (such as the 99 th percentile) is enough to remove all of them.
		Very long tracks that are likely due to background signals	These trajectories can be excluded from the analysis by using the ROI selection tools (Step 57).
47	Small track numbers	Inadequate parameters for spot detection	Check the detection quality with sptPALM_viewer visualization tools (Step 49) and modify detection parameters in MTT (e.g. threshold)
			Check the Gaussian distribution of spots and adapt the time integration of the camera if possible.
56-62	Small track length	Too high laser power for the excitation	Decrease 561 nm laser power. Note this will also decrease the Signal/Background ratio
60	High D values for control experiments with fixed mEOS on coverslips	Inappropriate acquisition time or pixel size	Check the camera acquisition time and pixel size and enter it in sptPALM_viewer (Step 46)
		Sample movement in XY or Z axis during time-lapse	Discard acquisition. Fiducial marker can be added on the coverslip (step 13) to correct drift in a post-acquisition treatment

		Poor signal/Background ratio	Increase the 561 nm laser power
--	--	------------------------------	---------------------------------

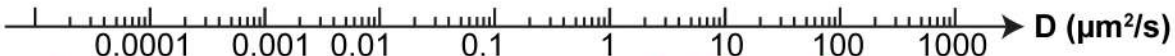


FRAP

FCS

sptPALM

SMdM

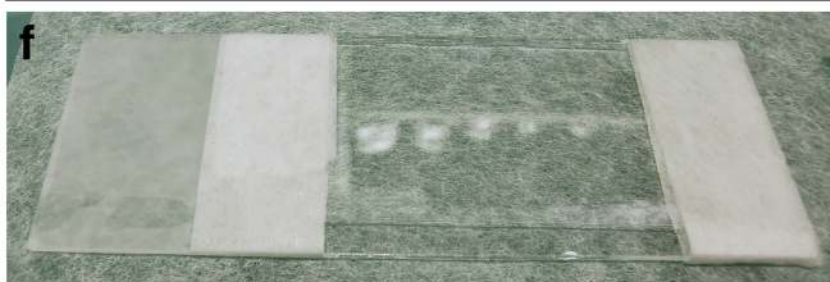
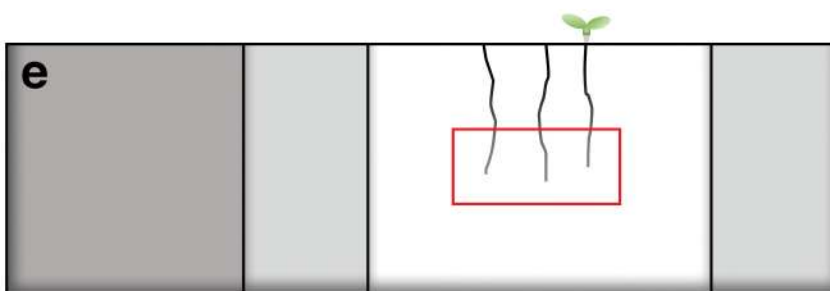
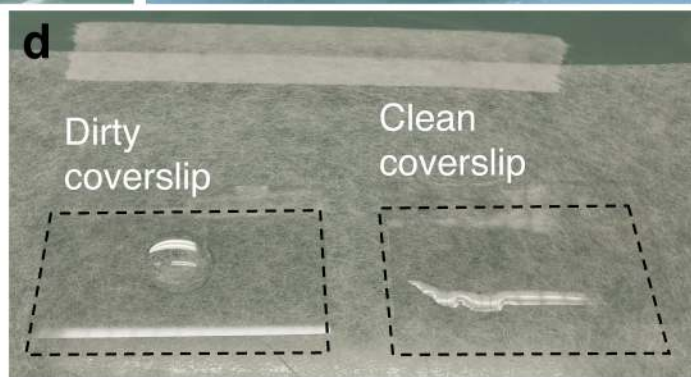
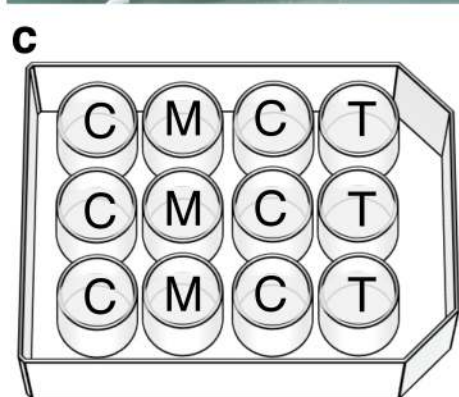
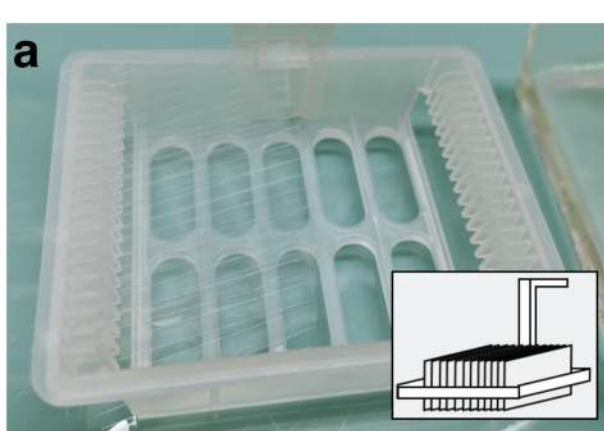


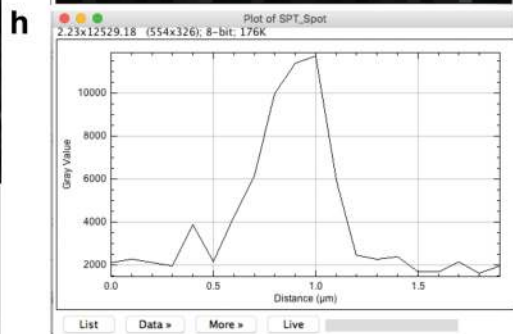
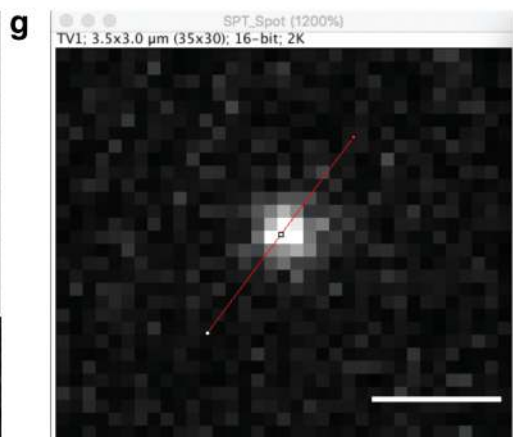
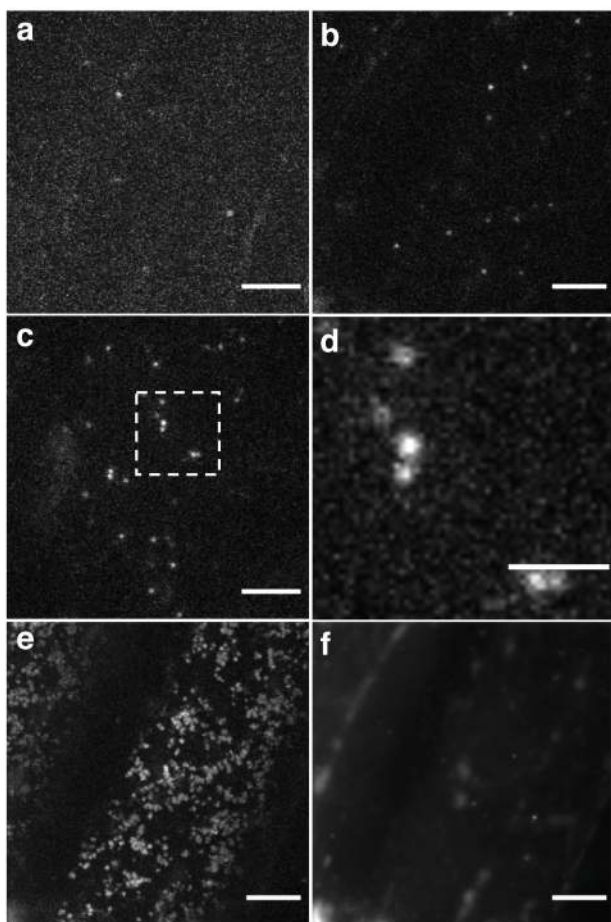
membrane proteins free cytosolic proteins

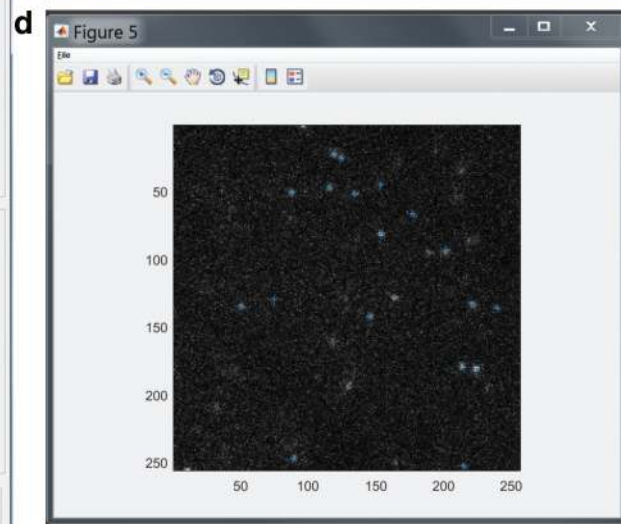
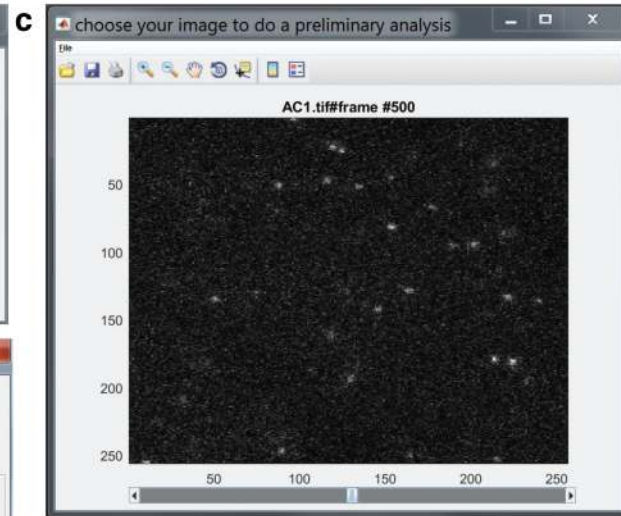
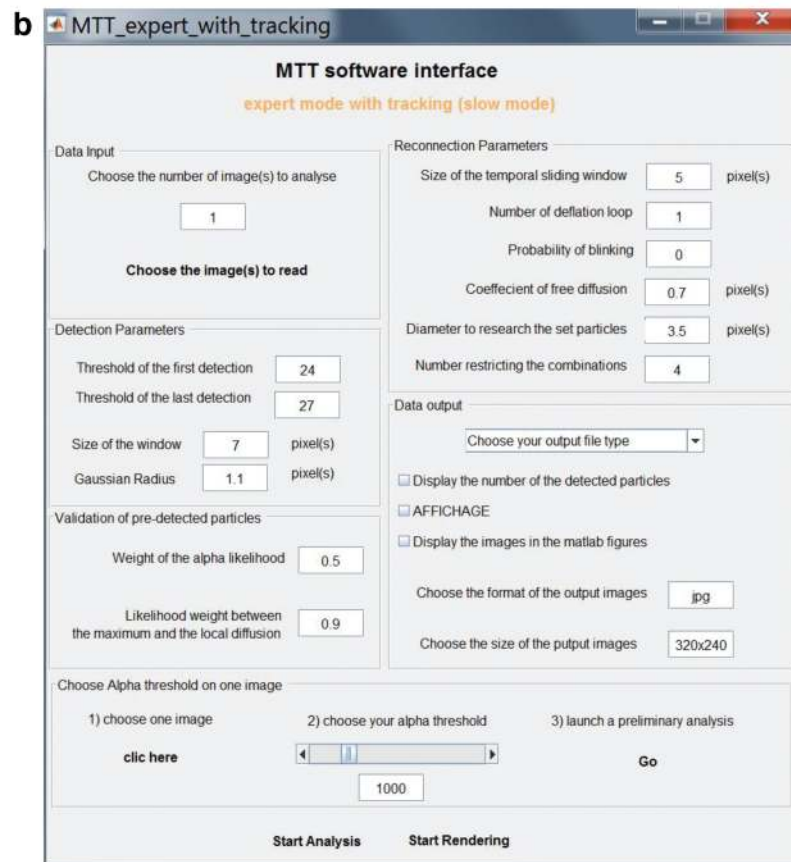
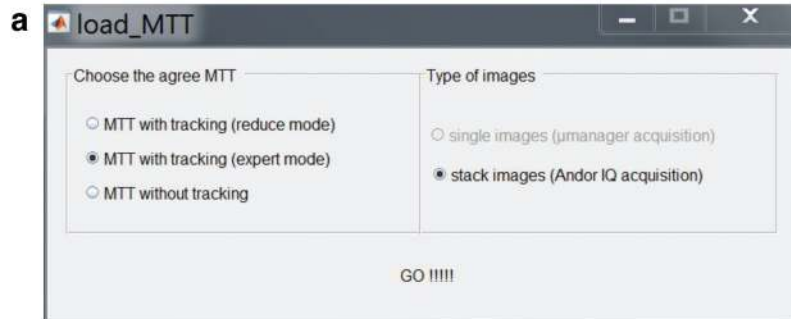
more confined
e.g. PIP2;1
AHA2

more mobile
e.g. LTI6B

diffusion of GFP in
aqueous solution







a sptPALM_Control_Panel

E:\TPbioscience\SPT-PALM\treated\EVECT2\EVECT2 mEOS a.lsm

Loading MTT data

Acquisition time (ms) Pixel size (um)

Saving file name Save all trajectories in txt file?

MTT

Analysis parameters

Maximum distance between two detections (um)

Maximum number of blinks (frames)

Minimum trajectory duration (frames)

Number of points used for D estimation

Maximum display time for MSD (s)

Method for the calculation of D :

Diffusion analysis

Plot trajectories

Statistics

Number of movies loaded Number of trajectories loaded

Number of trajectories after filtering Number of trajectories found in ROI

Number of trajectories used for Diff Density of tracks in ROI (um²)

Visualization tool

Select frame

Contrast (upper limit)

Contrast (lower limit)

First frame Last frame Movie title

Simulation of sptPALM experiments

Diffusion coeff #1 Diffusion coeff #2 Fraction of prot1 (%)

Number of frames

Display all images

